ARMY RESEARCH LABORATORY

Modal Analysis of the M113 Armored Personnel Carrier Metallic Hull and Composite Hull

Morris S. Berman

ARL-MR-246 August 1995

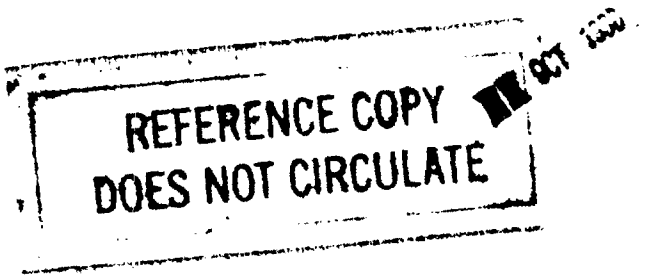

NOTICES

Destroy this report when it is no longer needed. DO NOT return it to the originator.

Additional copies of this report may be obtained from the National Technical Information Service, U.S. Department of Commerce, 5285 Port Royal Road, Springfield, VA 22161.

The findings of this report are not to be construed as an official Department of the Army position, unless so designated by other authorized documents.

The use of trade names or manufacturers' names in this report does not constitute indorsement of any commercial product.

REPORT DOCUMENTATION PAGE

Form Approved
OMB No. 0704-0188

1. AGENCY USE ONLY *(Leave blank)*	2. REPORT DATE	3. REPORT TYPE AND DATES COVERED
	August 1995	Final, July 1993 - February 1994

4. TITLE AND SUBTITLE
Experimental Modal Analysis of the M113 Armored Personnel Carrier Metallic Hull and Composite Hull

5. FUNDING NUMBERS
3H48H5

6. AUTHOR(S)
Morris S. Berman

7. PERFORMING ORGANIZATION NAME(S) AND ADDRESS(ES)
U.S. Army Research Laboratory
ATTN: AMSRL-WT-PD (ALC)
2800 Powder Mill Road
Adelphi, MD 20783-1197

8. PERFORMING ORGANIZATION REPORT NUMBER
ARL-MR-246

9. SPONSORING/MONITORING AGENCY NAMES(S) AND ADDRESS(ES)

10.SPONSORING/MONITORING AGENCY REPORT NUMBER

11. SUPPLEMENTARY NOTES

12a. DISTRIBUTION/AVAILABILITY STATEMENT
Approved for public release; distribution is unlimited.

12b. DISTRIBUTION CODE

13. ABSTRACT *(Maximum 200 words)*

An experimental comparative modal analysis was performed on a standard M113 armored personnel carrier and an experimental M113 armored personnel carrier. The objective of this experiment was to provide sufficient experimental data to validate survivability finite element models and to extract modeling parameters and information wherever appropriate.

This report details the results of the analysis performed on the data provided by the University of Cincinnati Structural Dynamics Research Laboratory. Each hull was tested in two configurations: a basic configuration consisting of the stripped hull, and a "tight-fitting" configuration consisting of the basic hull configuration to which dynamically linear behaving components, such as the engine, hatches, and doors, were attached to approximate a full-up vehicle.

The first elastic mode of the basic metallic hull was observed at 43.3 Hz (0.21% critical damping) while the first elastic mode of the basic composite hull was observed at 27.5 Hz (1.3% critical damping). Numerous local modes of varying degrees of complexity were observed for the tight-fitting configurations. This report describes the characteristics and peculiarities of all observed modes.

14. SUBJECT TERMS
M113 armored personnel carrier, modal analysis, vibration composite

15. NUMBER OF PAGES
51

16. PRICE CODE

17. SECURITY CLASSIFICATION OF REPORT	18. SECURITY CLASSIFICATION OF THIS PAGE	19. SECURITY CLASSIFICATION OF ABSTRACT	20. LIMITATION OF ABSTRACT
UNCLASSIFIED	UNCLASSIFIED	UNCLASSIFIED	UL

INTENTIONALLY LEFT BLANK.

ACKNOWLEDGMENTS

The author of this paper wishes to acknowledge the assistance of Jeff Poland and Dan Ryan of the Modal Shop in the conduction of this modal test. The author would also like to thank Professor Stuart Shelley of the University of Cincinnati for his assistance in the analysis portion of this project. Ting H. Li and Abraham Frydman of the Propulsion and Flight Division (PFD) of the U.S. Army Research Laboratory (ARL) furnished other technical assistance. The author also wishes to acknowledge Barbara Moore of the Weapons Concepts Division (WCD) and Dr. Joseph Santiago of the Terminal Effects Division (TED) who provided the funding and the insight into survivability modeling objectives and applications.

INTENTIONALLY LEFT BLANK.

TABLE OF CONTENTS

		Page
	ACKNOWLEDGMENTS	iii
	LIST OF FIGURES	vii
	LIST OF TABLES	ix
1.	INTRODUCTION	1
2.	METHODOLOGY AND BACKGROUND	1
3.	MODAL TEST CONFIGURATIONS	5
3.1	Vehicle Configurations	5
3.2	Vehicle Support System	6
3.3	Excitation and Data Acquisition System	6
3.4	Modal Model Geometry	9
4.	MODAL ANALYSIS RESULTS	9
4.1	General Description	9
4.2	Accuracy and Uncertainty	11
4.3	Basic Configuration, Aluminum Hull	12
4.4	Tight-Fitting Configuration, Aluminum Hull	17
4.5	Basic Configuration, Composite Hull	23
4.6	Tight-Fitting Configuration, Composite Hull	28
5.	CONCLUSIONS	33
5.1	Metallic vs. Composite Hulls	34
5.2	Basic vs. Tight-Fitting Configurations	34
5.3	Bradley Fighting Vehicle Comparison	35
	BIBLIOGRAPHY	37
	APPENDIX: FIRESTONE AIRMOUNT ISOLATOR DATA SHEET	39
	DISTRIBUTION LIST	43

INTENTIONALLY LEFT BLANK.

LIST OF FIGURES

Figure		Page
1.	Typical exciter-driving-point configuration	7
2.	Composite vehicle phase rolloff error	8
3.	Basic configuration geometry	10
4.	Tight-fitting configuration geometry	10
5.	Edge nomenclature	11
6.	Basic configuration, aluminum hull MMIF	13
7.	Basic configuration, aluminum hull driving-point FRFs	14
8.	Basic configuration, aluminum hull MAC matrix	14
9.	Basic configuration, aluminum hull, mode 6, 43.3 Hz	16
10.	Basic configuration, aluminum hull, mode 10, 81.2 Hz	16
11.	Tight-fitting configuration, aluminum hull MMIF	19
12.	Tight-fitting configuration, aluminum hull driving-point FRFs	19
13.	Tight-fitting configuration, aluminum hull MAC matrix	20
14.	Basic configuration, composite hull MMIF	25
15.	Basic configuration, composite hull driving-point FRFs	25
16.	Basic configuration, composite hull MAC matrix	26
17.	Basic configuration, composite hull, mode 7, 29.1 Hz	26
18.	Tight-fitting configuration, composite hull MMIF	30
19.	Tight-fitting configuration, composite hull driving-point FRFs	30
20.	Tight-fitting configuration, composite hull MAC matrix	31
21.	Tight-fitting configuration, composite hull, mode 16, 43.2 Hz	32

INTENTIONALLY LEFT BLANK.

LIST OF TABLES

Table		Page
1.	Vehicle Configurations Tested	5
2.	Recorded Air Pressure of Airmount Isolators	6
3.	Basic Configuration, Aluminum Hull Modal Parameters	13
4.	Tight-Fitting Configuration, Aluminum Hull Modal Parameters	18
5.	Basic Configuration, Composite Hull Modal Parameters	23
6.	Tight-Fitting Configuration, Composite Hull	29

INTENTIONALLY LEFT BLANK.

1. INTRODUCTION

A modal test and analysis were performed on the M113 armored personnel carrier by the Mechanics and Structures Branch (MSB) of the U.S. Army Research Laboratory (ARL). The modal analysis results will be used by the Terminal Effects Division (TED) of ARL for the validation of finite element models. These models will be used to assess the vehicles' survivability under munitions blast effects and impact from projectiles.

The modal test was carried out by the University of Cincinnati, Structural Dynamics Research Laboratory (UC/SDRL) under contract to the MSB. UC/SDRL acquired the modal data and performed a preliminary analysis to verify the data's integrity. The UC/SDRL also provided all portable test equipment required for the modal testing. This provision of the contract significantly reduced the cost of this test to the Government.

The data and preliminary analysis provided by UC/SDRL was transferred to the MSB for the completion of the modal analysis. This report presents the results of the complete modal analysis performed by the MSB.

2. METHODOLOGY AND BACKGROUND

The aim of a dynamic analysis is to determine the dynamic response of a structure to a defined forcing function. Traditionally the designer constructs a finite element (FE) model of the structure. This model is then discretized and represented by a stiffness matrix ([K]), a damping matrix ([C]), and a mass matrix ([M]). The sum of the forces introduced by these matrices is set equal to the forcing function (f(t)). In this report, square brackets ([]) will be used to represent matrices, and braces ({}) will be used to represent vectors. The basic equations of motion for the discretized model become

$$[M]\{\ddot{x}(t)\} + [C]\{\dot{x}(t)\} + [K]\{x(t)\} = \{f(t)\}. \tag{1}$$

For simplicity, equation (1) can be reformulated without the damping term in the Laplace domain as

$$s^2 [M]\{X(s)\} + [K]\{X(s)\} = \{F(s)\}. \tag{2}$$

The equations of motion are thus transformed from differential equations to algebraic equations in the Laplace domain. To solve for the resonant frequencies of the system, the forcing function is set to zero and equation (2) can be written

$$\left(s^2[M]+[K]\right)\{X(s)\}=0. \tag{3}$$

From linear algebra, the only nontrivial solution ($\{X\}\neq\{0\}$) of equation (3) is given by

$$|s^2[M]+[K]|=0. \tag{4}$$

Equations (3) and (4) can be reorganized into a standard eigenvalue problem as follows, where [I] represents the identity matrix,

$$\left[[K]^{-1}[M]+\frac{1}{s^2}[I]\right]\{X(s)\}=\{0\}. \tag{5}$$

From the form of equation (5), the characteristic equation of the discretized model is

$$\left(\frac{1}{s^2}\right)^n+a_1\left(\frac{1}{s^2}\right)^{n-1}+\ldots+a_{n-1}\left(\frac{1}{s^2}\right)^1+a_n=0. \tag{6}$$

In equation (6), s is a dummy variable for the complex valued modal frequencies ($\lambda_r = j\omega_r$, where ω_r is the r'th natural frequency and λ_r are the eigenvalues). For an n degree of freedom (DOF) system, there will be n complex modal frequencies (ω_r) and n complex modal vectors (Ψ_r), where the modal vectors are the eigenvectors. It is important to note that in a damped system, the eigenvalues will be complex quantities where the imaginary part is related to the damping factor.

Because a mathematical expression describing the dynamic properties cannot be obtained simply by visually inspecting a structure, experimental modal analysis techniques must be used to obtain the desired

properties such as modal frequency, shape, and damping, from the dynamic response measurements of the physical structure.

Assuming [M] and [K] are unknown and the system is undamped, then by letting

$$[B(s)] = s^2 [M] + [K]$$

and substituting into equation (2) the result is

$$[B(s)]\{X(s)\} = \{F(s)\}. \tag{7}$$

Defining a transfer function H(s) in matrix form

$$[H(s)] = [B(s)]^{-1} \tag{8}$$

equation (7) can then be written

$$\{X(s)\} = [H(s)]\{F(s)\}. \tag{9}$$

Matrix [H(s)] relates the force input of the system ({F(s)}) to the displacement response of the system ({X(s)}) and is commonly called the system's transfer function matrix.

A simple two-DOF system clarifies the physical meaning of the transfer function matrix.

$$[H(s)] = \begin{bmatrix} H_{11}(s) & H_{12}(s) \\ H_{21}(s) & H_{22}(s) \end{bmatrix} \tag{10}$$

Substituting equation (10) into (9) and expanding the result yields

$$H_{11}(s)F_1(s) + H_{12}(s)F_2(s) = X_1(s) \qquad \text{(a)}$$

$$H_{21}(s)F_1(s) + H_{22}(s)F_2(s) = X_2(s). \qquad \text{(b)} \tag{11}$$

If one forcing function, say F_2, is set to zero then

$$H_{11}(s) = \frac{X_1(s)}{F_1(s)} \quad \text{(a)} \qquad H_{21}(s) = \frac{X_2(s)}{F_1(s)}. \quad \text{(b)} \tag{12}$$

Or, with the p'th output DOF and the q'th input DOF, equation (12) is expressed in generalized notation form as

$$H_{pq}(s) = \frac{X_p(s)}{F_q(s)}. \tag{13}$$

If the system is excited at location q by the forcing function $F_q(s)$ and the output is measured at location p as $X_p(s)$, then $H_{pq}(s)$ is the measured transfer function between the input and output points. A more comprehensive discussion can be found in Allemang.[1]

Experimental modal analysis obtains the system's modal parameters (e.g., frequency and damping) by reconstructing the entire transfer function matrix from a single row or column of the system's measured transfer functions. In order to increase accuracy and provide the ability to extract double modes, several rows or columns are typically measured and the results are curve fit by a least-squares modal curve fitter. Because of the number of modes and desired degree of accuracy, a multiple DOF polyreference curve fitter was chosen for this analysis.

The Structural Dynamics Research Corporation (SDRC) software which was utilized for the modal analysis provides a time domain polyreference modal curve fitter. This curve fitter relies on an algorithm very similar to the complex exponential algorithm. The frequency response function matrix (identical to

[1] Allemang, R. J. "Vibrations: Analytical and Experimental Modal Analysis." UC-SDRC-CN-20-263-662, University of Cincinnati, Structural Dynamics Research Laboratory, Cincinnati, OH, 1992.

the transfer function matrix) is inverse Fourier transformed into the time domain. The result of the inverse transformation is the system's impulse response functions. Each of the impulse response functions is assumed to be the sum of several exponential terms, where each term contains the frequency and damping parameters of a single mode. A least-squares curve fit is then used to minimize the error between the experimental data and the exponential terms containing the modal parameters. A detailed description of this algorithm is presented in the "SDRC I-DEAS Users Guide: Test."[2]

3. MODAL TEST CONFIGURATIONS*

3.1 Vehicle Configurations. Modal modeling is much more effective if performed in stages. Initially, the model should consist of the simplest possible configuration and then progress to more complex configurations. As a result of this modeling strategy, two configurations of each M113 hull were tested. The "basic" configuration consisted of the bare M113 hull with all components removed. The "tight-fitting" hull consisted of the bare configuration with several major linear components attached. A linear component exhibits a response which is directly proportional to the force which is exciting it. The components were chosen for the tight-fitting configuration on the basis of mass, similarity to a full-up vehicle, and a qualitative judgment of the linearity. The tested configurations and associated weights are listed in Table 1.

Table 1. Vehicle Configurations Tested

Configuration	Hull Material	Weight (lb)	Attached Components
Basic	Aluminum	7,540	None
	Composite	7,600	
Tight-Fitting	Aluminum	12,910	Engine/Transmission, Final Drive Casings, Cargo Hatch, Rear Ramp, Commander's Hatch, Driver's Hatch, Engine Cover, Top Cover
	Composite	12,710	

[2] Structural Dynamics Research Corporation. "SRDC I-DEAS Users Guide: Test." Cincinnati, OH, 1990.

* This section summarizes the University of Cincinnati Structural Dynamics Research Laboratory's report "Advanced Shock Impact Mechanics Methodology for Armored Fighting Vehicles: Experimental Modal Analysis Data Acquisition for Composite and Aluminum Hull M113 Armored Personnel Carriers." University of Cincinnati, Cincinnati, OH, 1993.

The metallic hull is officially identified as an M113A2 "Carrier Personnel Full Track Armored." The UID number is C4001MAA and the serial number is 12A74669. Since the composite hull is unique, no similar identifying marks are supplied.

3.2 Vehicle Support System. In order for the FE analyst to compare the model to the experimental modal model, the model's boundary conditions must match the test configuration. A quasi-free-free boundary condition for the experimental analysis has been shown to correlate well with FE models. This experimental boundary condition is achieved by suspending the vehicle such that the modes of the support system do not interfere with the flexible modes of the vehicle. Generally, the flexible modes of the vehicle can be considered decoupled from the modes that are caused by the supports if the frequency of the lowest flexible mode is greater than a factor of 3 or more of the highest rigid-body mode.

Each configuration of the M113 was suspended by four Firestone Airmount Isolators. This support mechanism provided the modal separation necessary to isolate the flexible modes from the rigid-body modes (RBM). The stiffness of the airmount isolators varies with their pressure (details regarding the RBM frequencies follow later in this report). A data sheet and record of the isolator's pressures throughout the test are given in the University of Cincinnati report. For the reader's convenience the pressure table is replicated in Table 2 and a data sheet appears in Appendix A.

Table 2. Recorded Air Pressure of Airmount Isolators

Test Configuration		Air Pressure (psi)			
		Front Left	Front Right	Rear Left	Rear Right
Aluminum	Basic	30	30	30	30
	Tight-Fitting	30	48	30	30
Composite	Basic	30	30	30	30
	Tight-Fitting	31	48	25	28

3.3 Excitation and Data Acquisition System. All configurations of the M113 vehicles were excited by four MB Dynamics Model 50 electromagnetic shakers rated at 50 lb of force. The four shakers were located at the four corners of the vehicles and oriented vertically along the bottom. This excitation location provided good excitation of global vehicle modes. The front two shakers were attached to the

vehicle directly beneath where the main drive axles exit the chassis and the rear two shakers were attached to the chassis which overhangs the tracks. The force applied by these exciters was measured by PCB model 208A02 piezoelectric force transducers.

These force transducers are extremely sensitive to side and torque loads. Experience has shown that the use of a long, thin stinger alleviates inaccurate measurements caused by torsion on the transducer. Therefore, the force transducers were attached to each shaker by a stinger. The force transducer was then attached directly to the hull. At each force input location a PCB piezoelectric accelerometer provided the driving-point response acceleration measurement. Figure 1 shows a typical exciter-driving-point location.

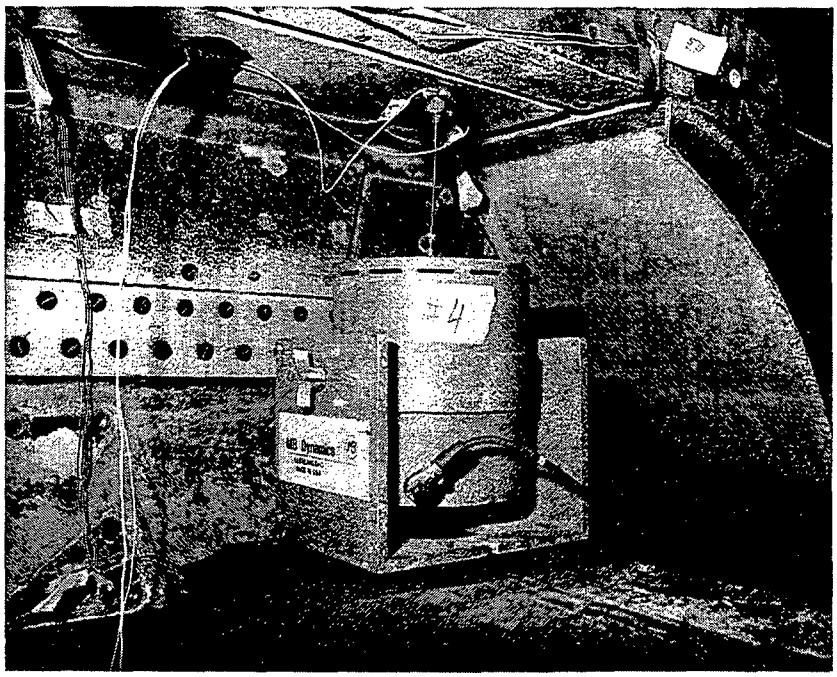

Figure 1. Typical exciter-driving-point configuration.

The response of the basic M113 configuration was measured at approximately 230 DOF, and approximately 350 DOFs were used to measure the tight-fitting configurations. The DOF locations were chosen to provide adequate spatial resolution based on past experience. PCB model 336C31 Flexcell accelerometers were used to measure the response of the lower portion of the vehicles. PCB model 336B31 and 336A31 Flexcells were used to measure the remainder of the response DOFs. All transducers were calibrated at UC/SDRL prior to arrival at the test site.

The data acquisition was performed on a 72-channel HP3565 data acquisition front end attached to an HP380 host work station. The response signals were routed through two 128-channel PCB data

harvesters which provided signal conditioning and automated patching. Four patches were required for the basic configuration and six patches were required for the tight-fitting configuration. LMS Cada-X software was utilized to provide the data acquisition support.

The multiple-input H1 method of frequency response function (FRF) calculation was utilized to reduce response measurement noise. The FRFs were calculated using 2,048 time points and approximately 100 averages. For the basic configuration, two FRFs were acquired at each DOF. The first FRF ranged from 0 Hz to 128 Hz and the second from 100 Hz to 228 Hz. Only one FRF from 0 Hz to 128 Hz was acquired for the tight-fitting configuration due to the high modal density. The resulting frequency resolution of these FRFs is 0.125 Hz. These FRFs include all calculated Fourier Transform lines, and thus the upper 20% of the frequency range is affected by aliasing errors.

After the data had been acquired and the analysis had begun, an error in the composite hull configuration's measurements was discovered. A mismatch between the response channels' and force input channels' analog filters resulted in a phase rolloff on all of the nondriving-point response measurements. The rolloff is approximately linear from 0° at 0 Hz to 85° at 228 Hz and is visible in Figure 2. Upon discovery, a correction factor was applied to all of the composite response measurements and the data was reanalyzed. The correction factor was obtained by inverting the phase characteristics of the filters.

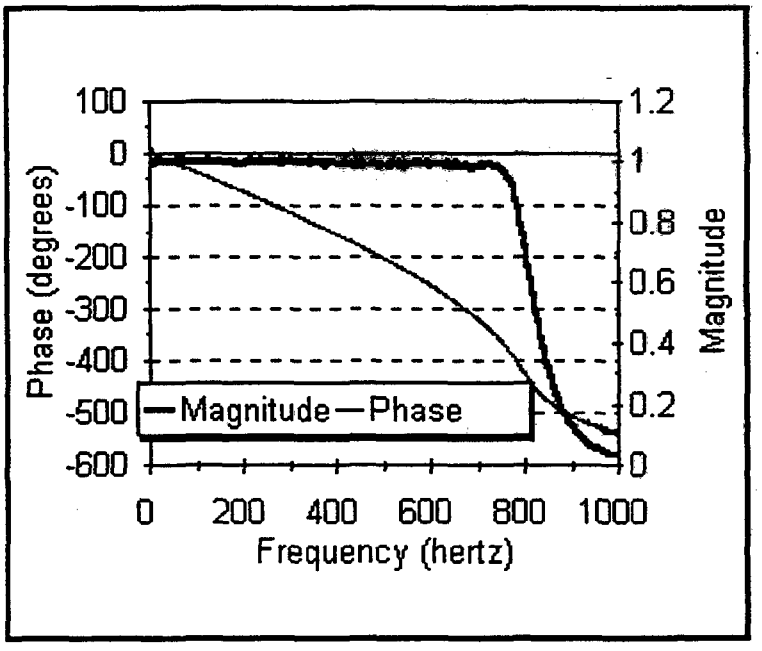

Figure 2. Composite vehicle phase rolloff error.

All configurations were excited using the burst random method. For the basic configurations, the vehicle was excited for 50% of the block time. For these configurations, an exponential window (e^{-Pt}, P = 0.2) was utilized to minimize leakage errors. A burst duration of 70% was utilized for the tight-fitting configurations. The bandwidth of the excitation was identical to the bandwidth being measured.

3.4 Modal Model Geometry. As stated earlier, the DOF locations were chosen to provide adequate spatial resolution for the modal model. Since the aluminum and composite hulls are extremely similar, the same geometry was utilized for the two hulls in both the basic and the tight-fitting configurations.

The X axis runs longitudinally along the vehicle from back to front. The Y axis is oriented laterally from right to left, and the Z axis is vertical from bottom to top. The origin is located in the middle of the rear edge of the floor of the M113. The geometry for the basic configurations is represented in Figure 3 and for the tight-fitting configurations in Figure 4.

4. MODAL ANALYSIS RESULTS

4.1 General Description. All parameter extraction and analysis was performed on a DECstation 5000/120 utilizing SDRC I-DEAS TDAS modal software. The polyreference method of parameter extraction was utilized.

The M113 is a complex structure. As a result, three-dimensional motion of this structure is difficult to convey in a two-dimensional medium. An arbitrary nomenclature has been assigned to assist in describing the motion of the vehicle. The edges are numbered from 1 to 4 which corresponds to the edges along the floor and ceiling. A letter is used to indicate the side of the vehicle on which the edge is located. Figure 5 details the assigned edge nomenclature. The mode shapes will also be available in an electronic format.

A representation of the modal assurance criterion (MAC) matrix is shown for each set of extracted mode shapes. Ideally, the value of the diagonal points will be 1 and the value at all of the other points will be zero. If a nondiagonal element's value is near 1 then those two modes of this model may be linearly dependent upon each other. However, if the modal model does not provide adequate spatial resolution, two modes may appear to be linearly dependent even if they are actually independent modes of vibration.

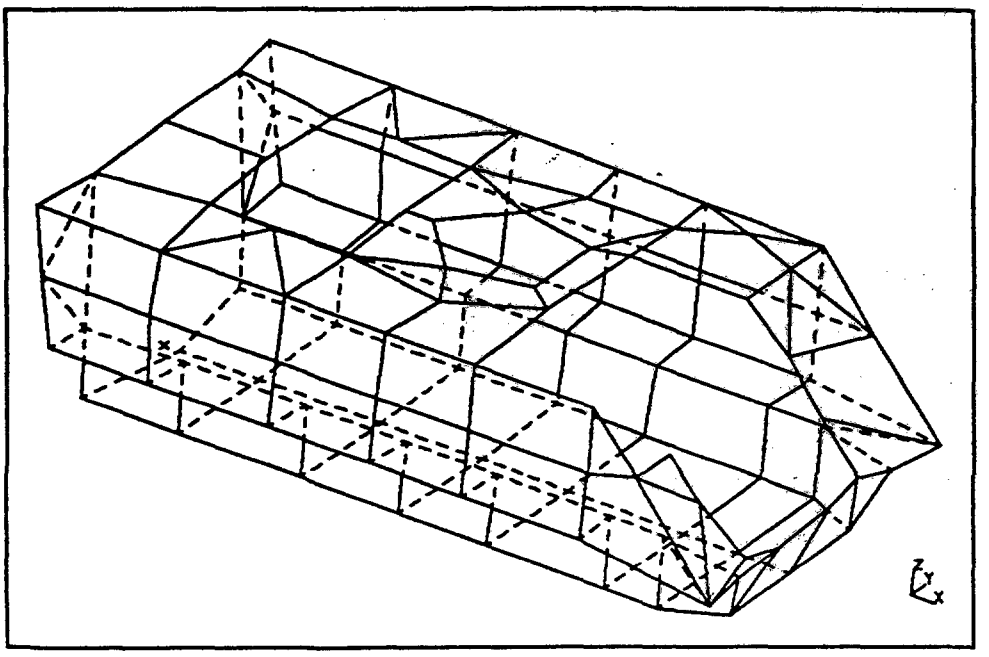

Figure 3. Basic configuration geometry.

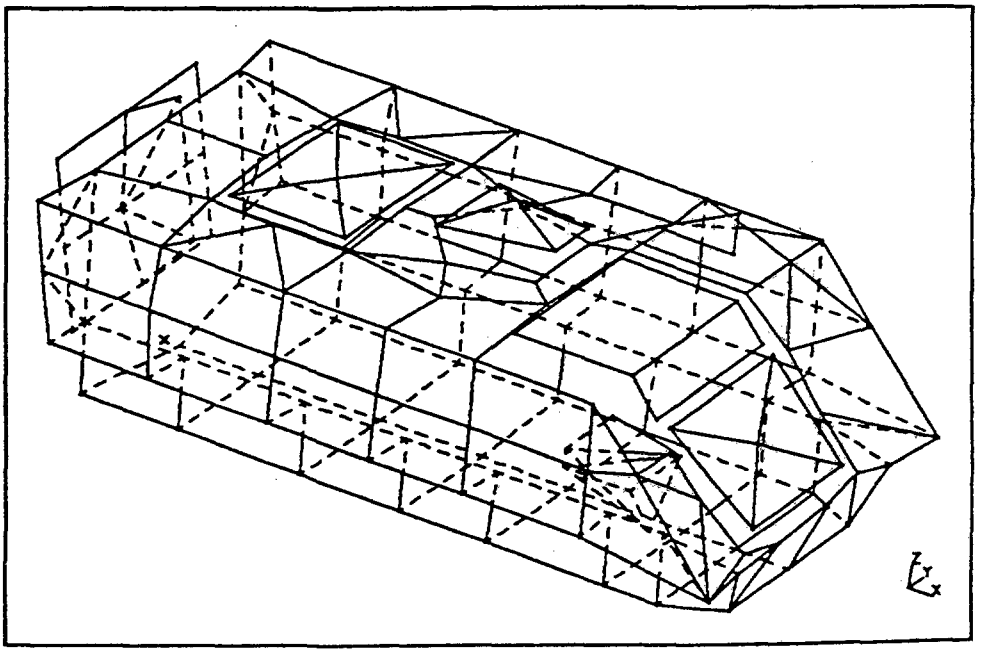

Figure 4. Tight-fitting configuration geometry.

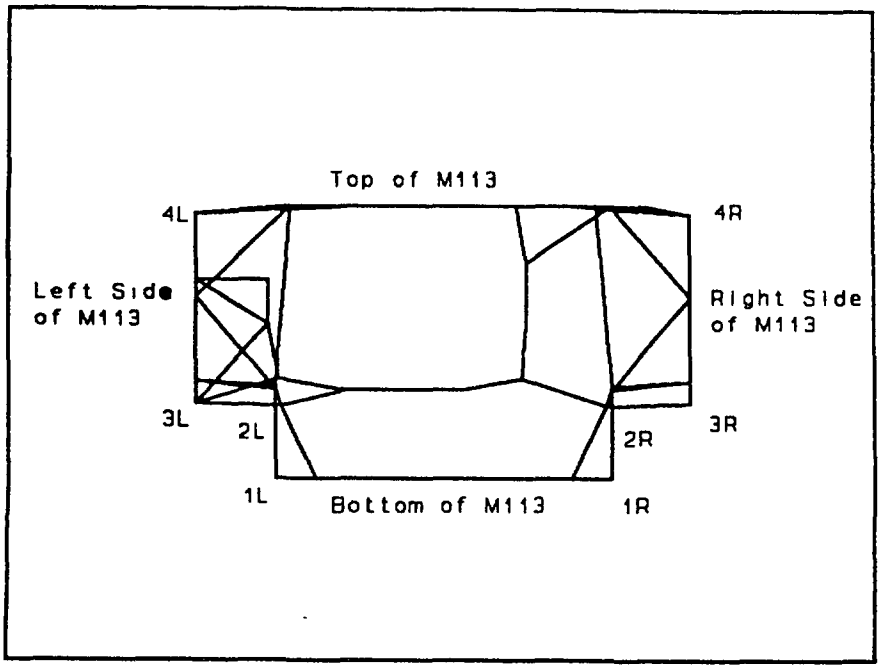

Figure 5. Edge nomenclature.

4.2 Accuracy and Uncertainty. The accuracy of uncertainty of estimated modal parameters is highly dependent on the structure being tested as well as the analysis parameters utilized. Structures with sharp, distinct resonances permit extraction of modal parameters with a high degree of accuracy. As the structural complexity increases and modes become coupled and more highly damped, it becomes increasingly more difficult to obtain accurate modal parameter estimates.

The accuracy of the modal parameters varies with each configuration and the frequency of each mode. For a well-excited ideal structure with low modal density and light damping, the frequency parameter estimates are accurate to fractions of a percent and the damping estimates are accurate to within 1%. In this experiment, the M113 is not an ideal vehicle. The accuracy estimates for these structures are based on the analyst's experience in conjunction with convergence criteria.

The stripped configuration of each hull provides the most accurate modal parameter estimates. The frequency estimates of the first several elastic modes of the basic configurations are accurate to within 5%. The damping estimates have a 10% accuracy. As the frequency increases, the accuracy with which modal parameters can be estimated decreases. In addition, as the modes become higher in frequency and more tightly coupled, the damping factor becomes extremely difficult to accurately estimate. The modal

parameter estimates for the composite hull are not quite as accurate as the aluminum hull due to the phase shift error in the measurement process.

The tight-fitting configuration of each hull provides accurate modal frequencies for the first several modes as well. However, since many of these modes are dependent on the interactions of the various added components, the modal parameters are extremely sensitive to the condition of the sealing surfaces and the torque with which the components are attached. The estimates of the damping parameters for the tight-fitting configuration are not as accurate as those for the basic configuration.

4.3 Basic Configuration, Aluminum Hull. The first configuration which will be discussed is the aluminum basic configuration. This configuration utilized a basic hull which had been subjected to minor shock tube damage. As a result of this damage, one of the rear mud guards was bent out of shape. The hull was inspected prior to the modal test; and MSB, in conjunction with TED, determined that the damage would not have a significant effect on the results of the modal analysis.

The modes in this configuration are minimally coupled and well separated. This fact is visible by viewing the multivariate mode indicator function (MMIF) in Figure 6. Minima of the curves in an MMIF represent the presence of a resonant frequency. In addition, the first flexible mode is visible at over 40 Hz and the highest rigid-body mode (RBM) is visible below 10 Hz. This separation provides more than the 1:3 ratio required to decouple the dynamics of the support structure from the dynamics of the vehicle.

Table 3 details the extracted modal parameters. Although data was collected up to 228 Hz, the inability to perform a convergent curve fit resulted in only modes up to 115 Hz being extracted. All four driving-point FRFs appear in Figure 7. Figure 8 is a representation of the MAC matrix from the mode shapes generated for this configuration.

Modes 1–5. Modes 1 through 4 are the extracted RBMs. Although there is a maximum of six RBMs, only three could be extracted due to noise in the FRFs. In modes 1 and 2, the hull rolls about its longitudinal axis. The center of rotation is different for each of these modes. Modes 3 and 4 are both vertical heave modes. In mode 3 the forward portion of the hull bends upward slightly. Mode 5 is the hull pitch mode where the hull rotates about its transverse axis.

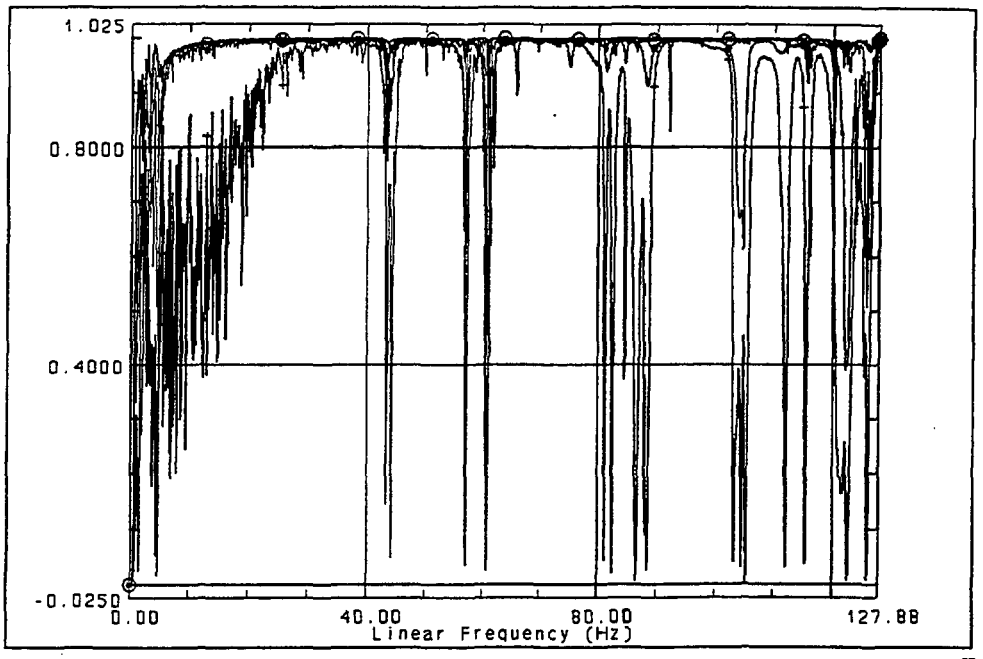

Figure 6. Basic configuration, aluminum hull MMIF.

Table 3. Basic Configuration, Aluminum Hull Modal Parameters

Mode No.	Frequency (Hz)	Damping (percent critical)	Mode No.	Frequency (Hz)	Damping (percent critical)
1	1.3	0.70	11	82.5	0.15
2	1.3	2.30	12	84.6	0.11
3	2.9	3.30	13	86.7	0.47
4	3.0	2.25	14	88.5	0.29
5	4.6	2.68	15	103.2	0.22
6	43.3	0.21	16	104.5	0.22
7	44.2	0.29	17	105.3	0.38
8	57.1	0.16	18	112.1	0.23
9	60.8	0.15	19	115.4	0.20
10	81.2	0.17	20	115.4	0.21

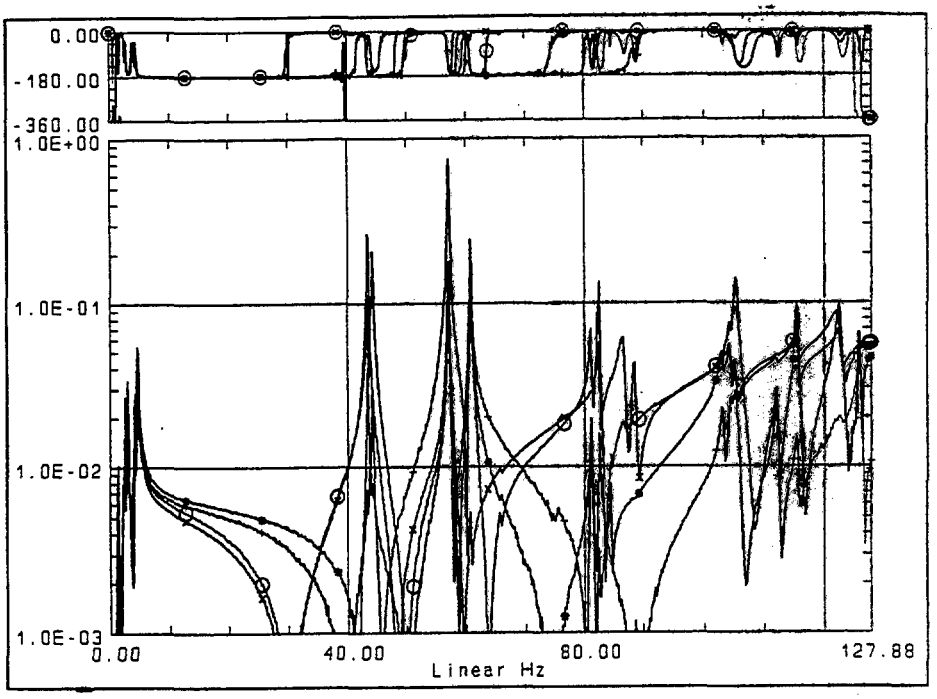

Figure 7. Basic configuration, aluminum hull driving-point FRFs.

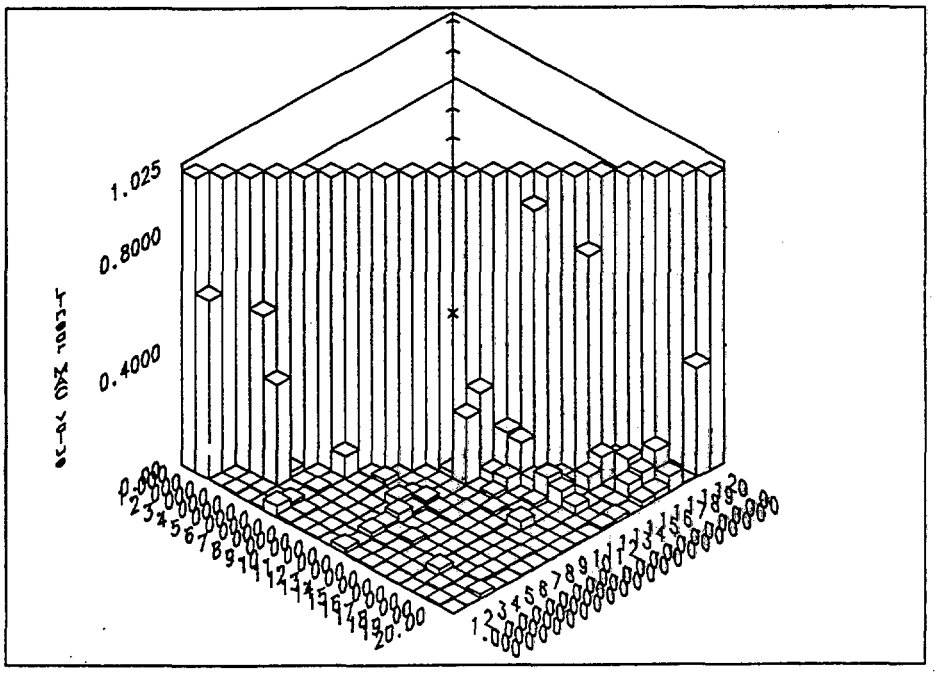

Figure 8. Basic configuration, aluminum hull MAC matrix.

Modes 6–7. Modes 6 and 7 are flexible modes which primarily show the deflection of the roof centered over the commander's hatch and the cargo hatch. Mode 6 (Figure 9) incorporates a slight torsional mode of the floor.

Modes 8–9. Mode 8's largest deflection is located in the roof with a twisting of the panel between the cargo hatch and the rear of the vehicle. In addition to this motion, the floor and the front of the vehicle are undergoing torsion. Mode 9 is similar to mode 8, however, the torsional portion of the mode is more pronounced. In addition, the two rearmost sections of the roof are moving with large amplitude out of phase with each other.

Modes 10–11. The center of the floor is bowing outward (Figure 10). Edges 1L, 2L, 3L, 1R, 2R, and 3R bow inward, resulting in a "squeezing" of the interior of the vehicle. The left and right sides of the roof move vertically 180° out of phase. Mode 11 is extremely similar to mode 10.

Mode 12. Mode 12 has roof motion similar to mode 11. Edges 1L and 2L bow upward while edge 3L and 4L bow downward. Edge 4L also bows inward slightly as it bows down. The right side of the vehicle exhibits the same motion as the left, however, the two sides are out of phase with each other.

Modes 13–16. The motion of the roof is again similar to mode 11. The left side panel of the vehicle is depressed inward while the right side panel is depressed outward. The center of the floor is depressed downward. Mode 14 is similar to mode 13, however, both are depressed inward simultaneously while the floor bows downward. Mode 15 is similar to mode 13, however, edges 4R and 4L remain somewhat stationary while the sides bow outward. Edge 4R is not stationary at the forwardmost part where it is not attached to anything. Mode 16 is related to mode 15 as mode 14 is related to mode 13. The sides move inward toward each other, essentially squeezing the vehicle.

Mode 17. Edges 1R and 3R move together while edges 1L and 3L move apart. The roof section between the front of the vehicle and the commander's hatch moves upward with the roof section just to the rear of the cargo hatch. The roof section between the cargo hatch and commander's hatch moves downward. The rear edge of the roof remains stationary.

Mode 18. The entire roof area surrounding the commander's hatch moves upward while the rear edge of the cargo hatch moves downward and the rear edge of the roof moves upward. The forward part of

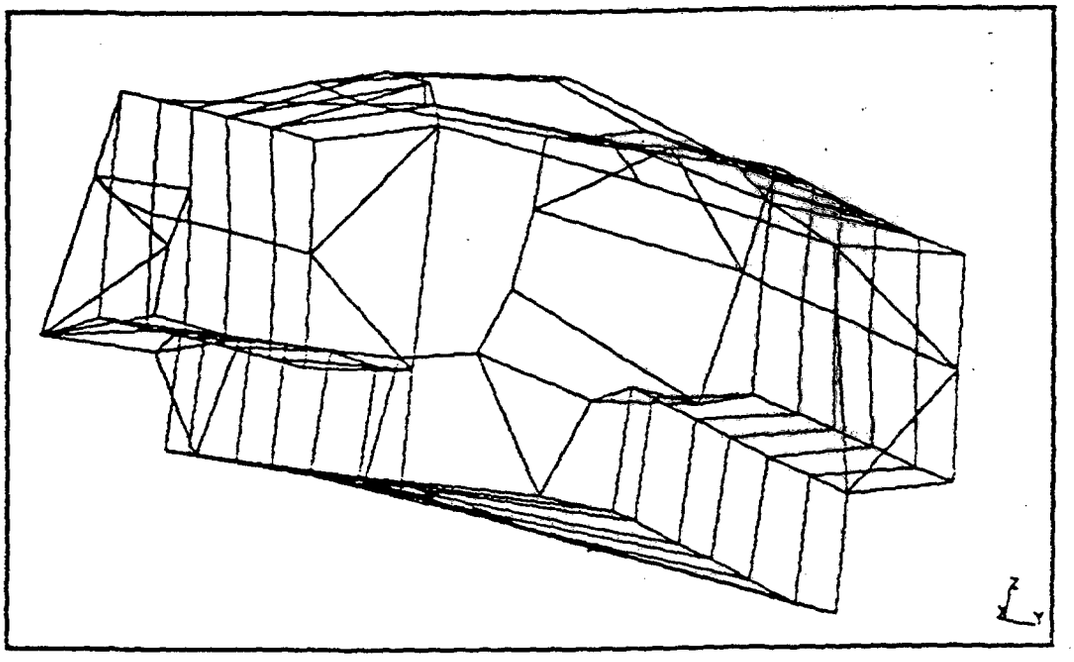

Figure 9. Basic configuration, aluminum hull, mode 6, 43.3 Hz.

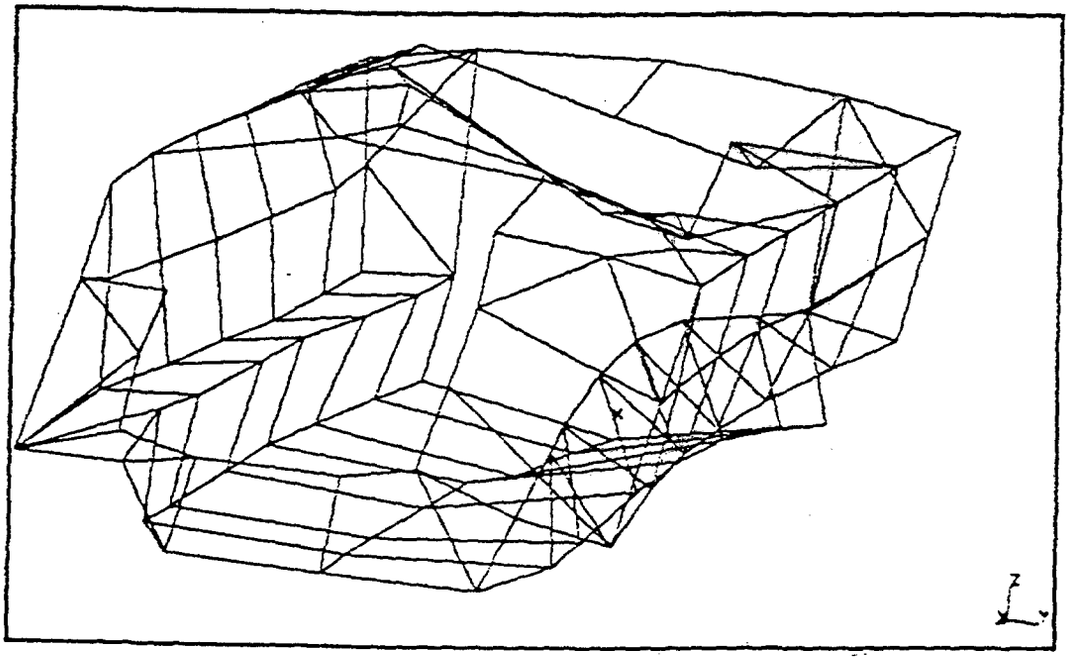

Figure 10. Basic configuration, aluminum hull, mode 10, 81.2 Hz.

the floor is arched upward and the rearward part is depressed downward. The sides exhibit minimal deflection in the z direction. However, edges 1R, 2R, 3R, 1L, 2L, and 3L move inward to squeeze the vehicle.

Modes 19–20. Edges 2L, 3L, and 4L form three corners of a square. In the middle of the vehicle, the square is rotated clockwise and down, while in the rear of the vehicle, it is rotating counterclockwise and up. The square formed by edges 2R, 3R, and 4R is rotating clockwise and down. The roof motion is similar to mode 18. The motion of the left side of the vehicle for mode 20 is similar to mode 19. The two sides in the front of the vehicle are rocking in toward each other and out away from each other at the rear.

4.4 Tight-Fitting Configuration, Aluminum Hull. This configuration utilized the same hull as the basic aluminum configuration. However, several tight-fitting components were added to the basic hull and are listed in Table 1. Table 4 details the extracted modal parameters for this configuration. Only modes up to 76 Hz were extracted. Above this frequency the modes become very highly coupled and extremely difficult to extract with reasonable accuracy.

The first elastic mode of this configuration is at 19 Hz, and the highest RBM is at 3.5 Hz. This provides enough separation of the flexible modes from the RBMs to decouple the modes of interest from the suspension system. Figure 11 shows the MMIF, and Figure 12 shows the driving-point FRFs for this configuration. Comparing the basic configuration MMIF (Figure 6) to this configuration's MMIF, the reader sees that the modal density is much higher. In addition, many more modes appear to be coupled. In the MAC matrix (Figure 13), several modes appear to be linearly dependent. Many of the modes extracted for the tight-fitting configuration involve variations on the motion of different hatches. This aspect of the vibration accounts for many of the high off-diagonal MAC values noted in Figure 13.

Modes 1–4. Mode 1 is the pitch RBM. The vehicles rotate about its transverse axis. Mode 2 is the vertical heave RBM. Mode 3 is another pitch mode. Mode 4 is the roll RBM.

Modes 5–6. Mode 5 has a slight flexible motion of the roof. The commander's hatch pivots in-plane about its right rear corner as the rear ramp rotates in-plane about its lower left corner. In mode 6, the rear ramp is rotating out-of-plane about its hinges, while the commander's hatch continues to rotate in-plane.

Table 4. Tight-Fitting Configuration, Aluminum Hull Modal Parameters

Mode No.	Frequency (Hz)	Damping (percent critical)	Mode No.	Frequency (Hz)	Damping (percent critical)
1	1.9	2.24	19	52.1	0.38
2	2.4	1.80	20	52.6	1.54
3	3.5	1.86	21	52.7	1.69
4	3.6	2.35	22	60.0	0.09
5	19.4	4.37	23	60.8	1.28
6	24.1	2.91	24	61.8	0.25
7	27.8	4.81	25	64.3	1.43
8	31.8	2.09	26	65.8	0.49
9	37.4	2.62	27	66.5	1.46
10	42.5	0.99	28	67.1	0.39
11	44.7	1.94	29	68.6	0.73
12	48.6	2.05	30	70.4	0.26
13	48.7	2.10	31	71.1	1.29
14	50.8	2.00	32	73.4	1.05
15	50.9	1.95	33	73.9	0.51
16	51.5	1.45	34	74.9	0.11
17	51.5	1.40	35	75.8	0.55
18	52.0	0.34	36	76.4	0.49

Mode 7. In mode 7, the engine and transmission rotate about a single point, while the cargo hatch rotates in-plane. The rear ramp also rotates slightly out-of-plane about its lower hinge.

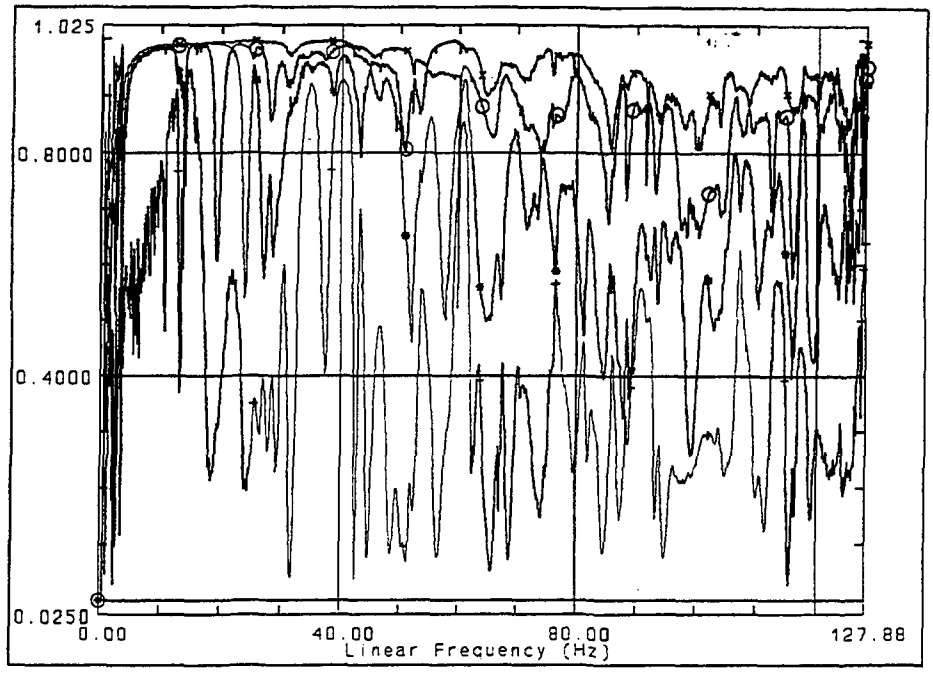

Figure 11. Tight-fitting configuration, aluminum hull MMIF.

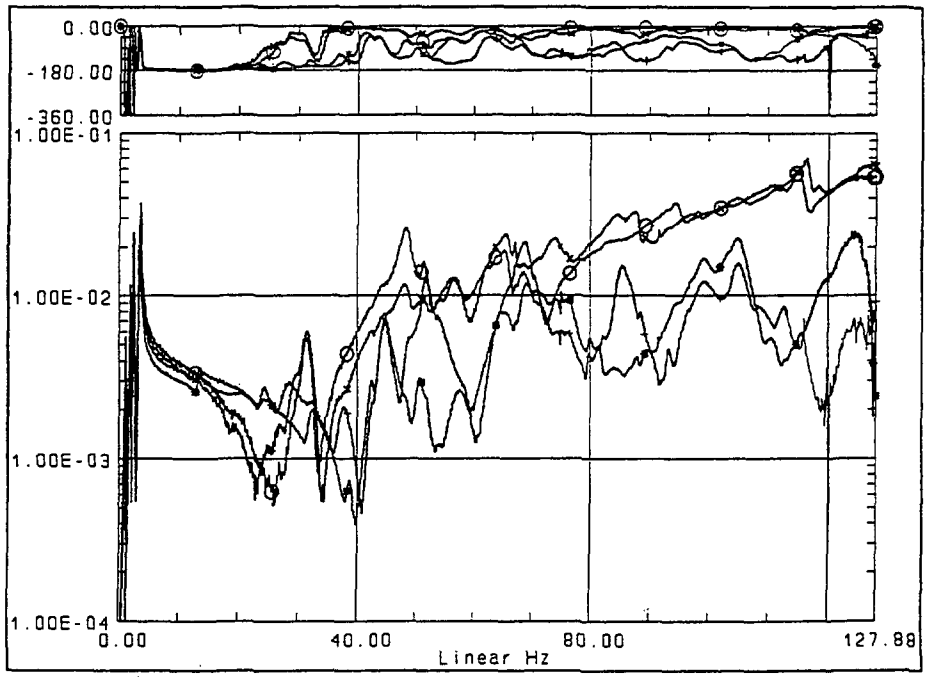

Figure 12. Tight-fitting configuration, aluminum hull driving-point FRFs.

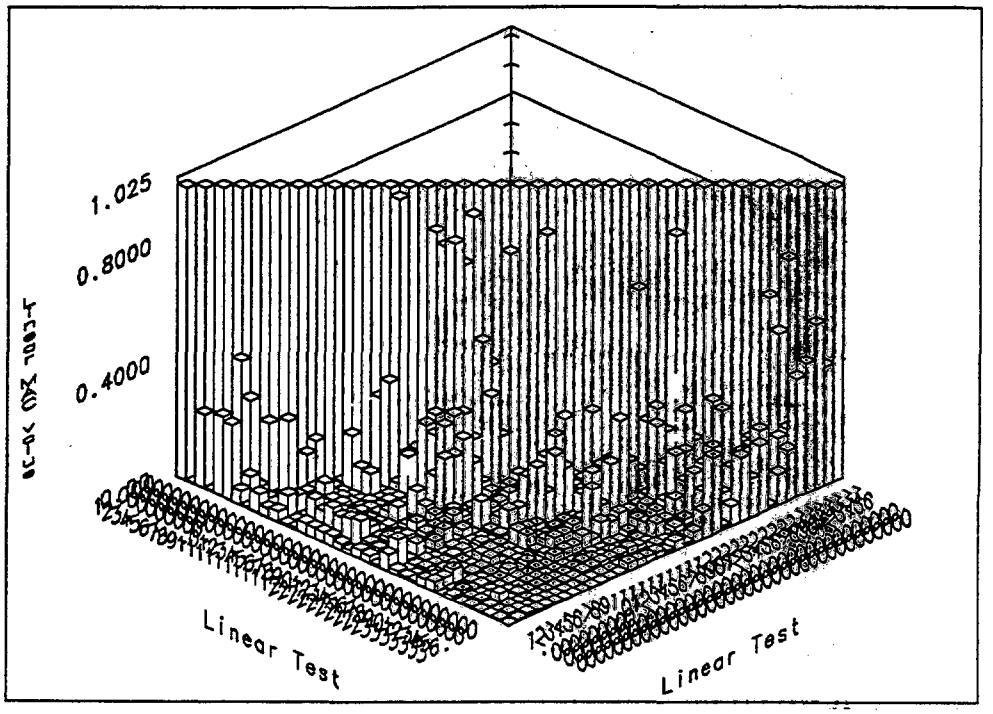

Figure 13. Tight-fitting configuration, aluminum hull MAC matrix.

Mode 8. The primary motion is a depression of the roof between the cargo hatch and the commander's hatch. The hatch motion merely follows the motion of the roof line.

Modes 9–10. The entire hull rolls along its longitudinal axis. The rear ramp bends and twists as the commander's hatch moves vertically. The engine/transmission unit rotates. Mode 10 is similar to mode 9, but is accompanied by a roof depression between the commander's hatch and cargo hatch. Mode 10 also lacks the rolling motion of mode 9. The top cover, engine cover, and driver's hatch also exhibit some motion.

Mode 11. Mode 11 is a torsional hull mode accompanied by significant hatch motion. The commander's hatch is translating vertically, as is the driver's hatch. The engine cover is rotating about its top left corner and the roof exhibits a slight depression. The engine is rotating and the rear ramp is translating and bending along the longitudinal axis of the vehicle. In addition, the rear ramp is rotating in-plane with the torsional motion of the hull.

Mode 12. Except for the roof, there is minimal flexible motion of the hull in this mode. The cargo hatch, engine cover, and top cover are rocking side to side. The roof flexes to accommodate this hatch motion.

Mode 13. The vehicle primarily deflects in a torsional manner. The hatches follow the displacement of the hull which surrounds them.

Modes 14–18. Most of the motion is generated by the roof and the associated hatches. The right side of the top cover is moving vertically with the largest displacement. The cargo hatch is rocking from side to side. Mode 15 is similar to mode 14; there is a much larger relative displacement between the cargo hatch and top cover. The hatch motions of mode 16 are similar to modes 14 and 15. A torsional displacement is also occurring. Mode 17 is again similar to mode 14, however, the commander's hatch exhibits much more relative displacement. In mode 18 the basic torsional motion is accompanied by edge 4L bowing outward. The cargo hatch rocks side to side while the driver's hatch rocks front to back. The commander's hatch moves front to back in-plane. The floor bows up and down while the engine moves vertically.

Mode 19. The left side panel of the vehicle is depressed inward while the forward part of the floor is also depressed inward. The cargo hatch rocks from side to side as the driver's hatch moves vertically.

Modes 20–21. The rear ramp rotates about a point behind the ramp. The commander's hatch and cargo hatch rotate about points above each hatch. The roof is depressed in the center between the commander's hatch and the cargo hatch. Mode 21 is almost identical to mode 20.

Mode 22. The motion is primarily on the right side of the hull. Edges 3R and 4R are deflecting inward while edge 1R deflects downward. The engine cover and commander's hatch are rotating out of plane.

Mode 23. This is largely a torsional mode. The engine cover rocks side to side while the engine, cargo hatch, and commander's hatch rock front to back. The door of the rear ramp exhibits some independent motion.

Modes 24–26. The hull remains stationary while the engine, engine cover, driver's hatch, and commander's hatch undergo displacement. The rear ramp rotates about its vertical axis with a large amplitude. The door in the ramp does not stay fixed to the ramp, but moves with a slightly higher amplitude. In mode 25, the hull remains stationary was well. The door in the rear ramp manifests quite a bit of motion as does the cargo hatch and the roof surrounding it. Mode 26 is similar to mode 25, with more motion of the right side of the vehicle. The plane defined by edges 1R and 2R moves upward and inward while the plane formed by edge 3R and 4R moves upward and outward.

Modes 27–28. There is a slight torsional motion in the rear of the vehicle. The rear ramp and the door in the rear ramp rotate about their vertical axes out of phase with each other. The engine cover and cargo hatch rock side to side in phase with each other. The roof moves in conjunction with the cargo hatch. Mode 28 also exhibits a slight torsional displacement. The motion of the cargo hatch and engine cover is similar to mode 27. The engine also rocks front to back.

Mode 29. The torsional motion from modes 27 and 28 is more pronounced. Edge 4L bows inward and downward. The plane defined by edges 3R and 4R twists inward and downward toward the front of the hull. The cargo hatch and commander's hatch rock side to side 180° out of phase with each other. The driver's hatch and the engine cover also rock side to side.

Mode 30. Edge 4L bows slightly inward and downward. The commander's hatch has a large vertical displacement. The cargo hatch rocks side to side. The front right of the engine cover and the rear right of the top cover have a large vertical displacement. The engine rocks on a diagonal.

Mode 31. The rear of the hull undergoes a slight torsional mode. The plane formed by edges 3R and 4R twists inward. Edges 1L and 2L bow upward and inward. Edge 3L bows inward. Edge 4L bows upward and outward. The driver's hatch translates side to side as well as rocks side to side. The engine cover and top cover also rock and translate side to side slightly.

Modes 32–36. The commander's and driver's hatches translate side to side. Most of the motion emanates from the door in the rear ramp and the rear ramp itself. Mode 33 is very similar to mode 32. Edge 1L bows downward slightly along with edge 2L. The cargo hatch and the engine and top cover translate and rock as well.

Mode 34. The commander's hatch and the driver's hatch exhibit most of the motion in mode 34. Edges 1L and 2L bow upward slightly. The front of the hull twists very slightly. Mode 35 adds motion from the rear ramp and rear ramp door. Mode 36 has the same hatch motion as mode 34, but adds in a torsional hull mode.

4.5 Basic Configuration, Composite Hull. The basic composite hull had not been subjected to any damage as the aluminum hull had been. The external surface of the composite hull was coated with a rubberized coating. The extracted modal parameters appear in Table 5.

Table 5. Basic Configuration, Composite Hull Modal Parameters

Mode No.	Frequency (Hz)	Damping (percent critical)	Mode No.	Frequency (Hz)	Damping (percent critical)
1	1.4	2.66	15	62.4	0.83
2	2.5	2.33	16	67.3	1.81
3	3.0	1.91	17	70.2	1.40
4	4.4	2.78	18	73.1	2.46
5	4.7	2.34	19	75.3	1.15
6	27.5	1.27	20	77.2	1.41
7	29.1	1.04	21	82.0	1.48
8	40.3	0.75	22	85.6	0.13
9	50.2	1.51	23	91.2	0.15
10	50.9	0.16	24	98.0	0.84
11	52.1	1.66	25	101.3	1.23
12	54.0	2.08	26	102.3	1.21
13	56.7	0.17	27	104.3	0.37
14	61.2	1.49			

The first flexible mode occurred at 27 Hz and the highest RBM occurs at 4.7 Hz. This provides enough separation between the RBMs and the elastic modes to prevent the suspension from affecting the elastic modes. For this configuration, only modes up to 104 Hz were extracted. Above this frequency the modes become very highly coupled and difficult to extract with accuracy. The MMIF appears in Figure 14. The four driving-point FRFs appear in Figure 15. The MAC matrix appears in Figure 16. Based on the MAC matrix modes 14 and 15 are extremely similar and may represent the same motion. Due to the higher material damping, there is more coupling of adjacent modes.

Modes 1–5. Mode 1 is a combined roll/translational mode. As the hull rolls it also translates along the Y axis. Mode 2 is a pitch mode. The motion of mode 3 is vertical heave. Mode 4 is a translation along the Y axis. Mode 5 is also a pitch mode.

Modes 6–8. There is a small torsional movement in the floor of the hull. The majority of the motion comes from the roof. Both front and rear edges of the cargo hatch opening move up and down in phase. Mode 7 (Figure 17) is a much more pronounced torsional mode. The top rear edge of the vehicle is rotating quite a bit. The right side of the vehicle also exhibits a slight depression. Mode 8 is also a torsional mode, however, there also a large pitching motion. The forward edge of the cargo hatch is bending up and down.

Mode 9. Edges 1L and 2L bend downward. Edges 3L and 4L bend outward. The plane formed by edges 3R and 4R rotates upward and inward, while a slight depression forms in that side. Both the front and rear edges of the cargo hatch bend upward.

Mode 10. Edges 1L, 2L, and 3L bend upward and inward. Edge 4L bends upward and outward. Edges 1R, 2R, and 3R bend downward and outward. Edge 4R bends inward. The middle of the right side of the hull is depressed. The rear edge of the cargo hatch bends downward, as does the front edge of the commander's hatch.

Modes 11–12. The midpoint between edge 3L and 4L flexes outward while the midpoint between edges 3R and 4R flexes inward. The left edge of the cargo hatch bends down and the right edge bends upward. In mode 12 edge 2L bows inward while edge 3L bows upward. Edges 1R and 2R bow down and edge 3R bows upward slightly. The roof motion is similar to mode 11.

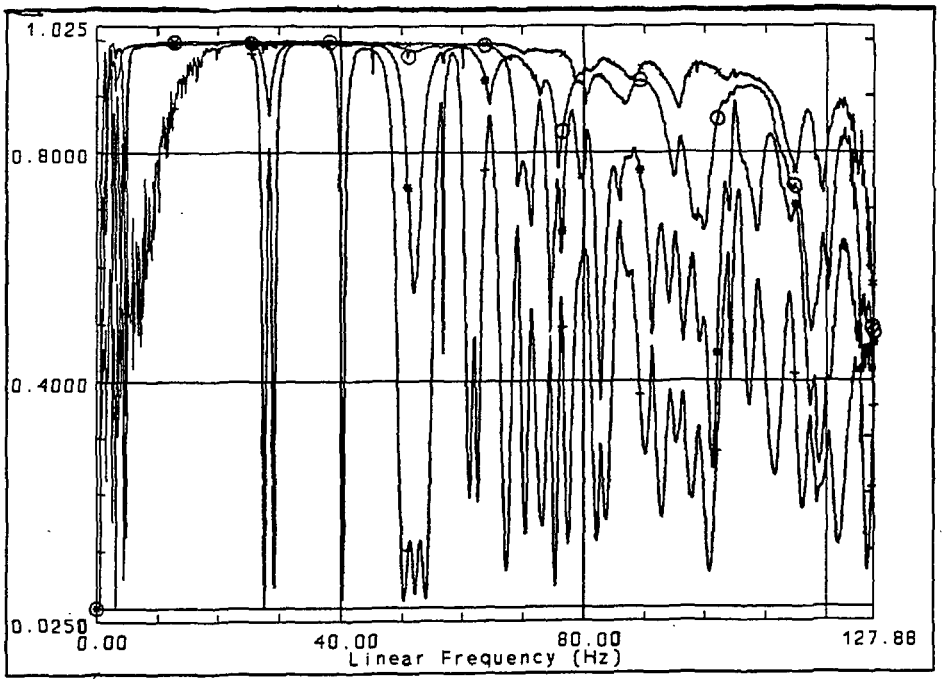

Figure 14. Basic configuration, composite hull MMIF.

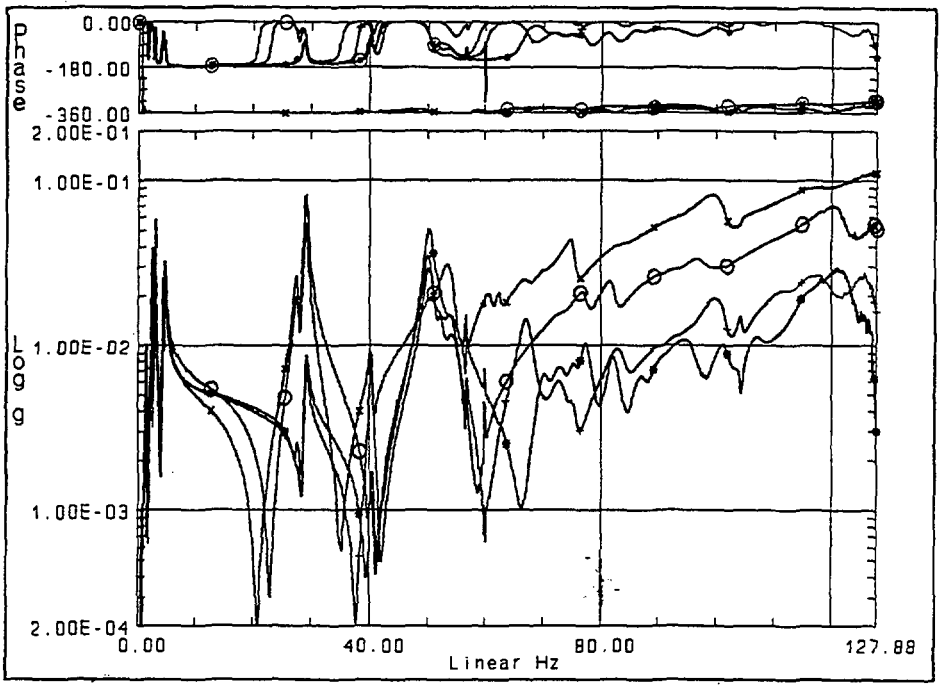

Figure 15. Basic configuration, composite hull driving-point FRFs.

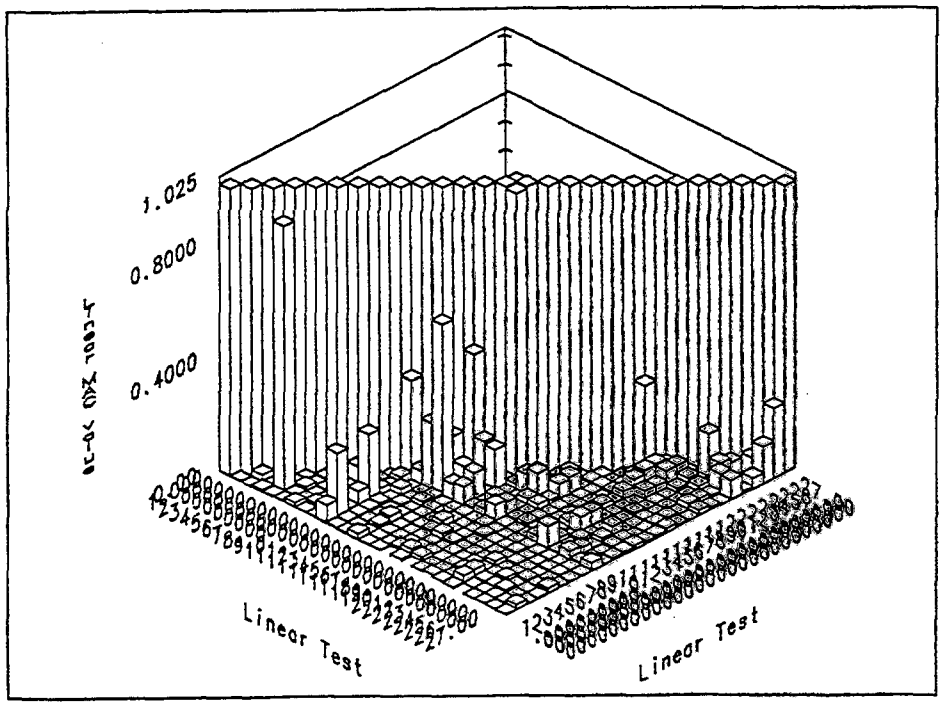

Figure 16. Basic configuration, composite hull MAC matrix.

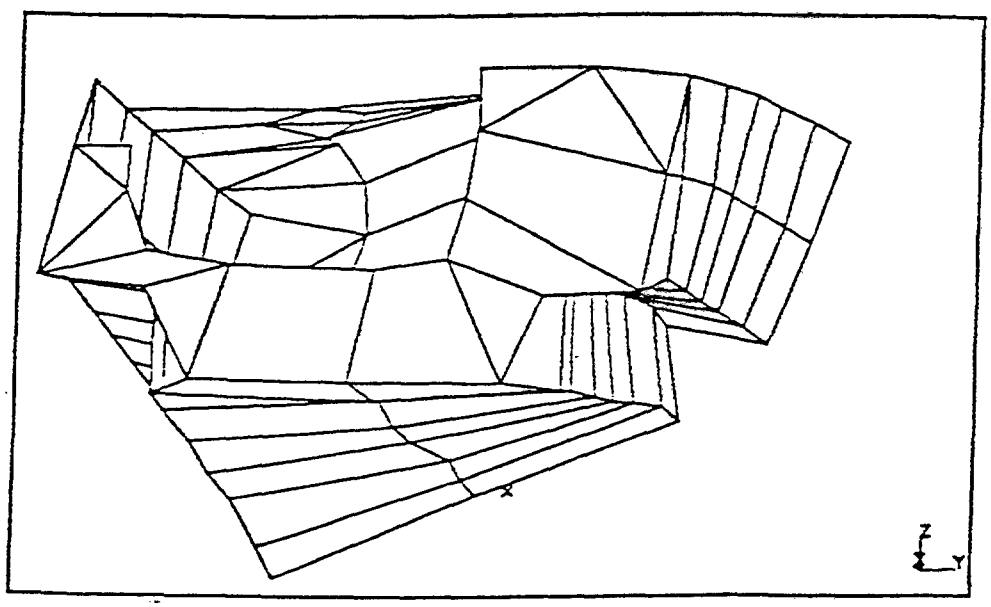

Figure 17. Basic configuration, composite hull, mode 7, 29.1 Hz.

Mode 13. There are many smaller motions in this mode. However, the overall displacement is the roof of the vehicle sliding laterally over the floor of the vehicle.

Modes 14–16. Edge 2L and 3L bow outward while edge 4L bows downward. There is a bubble in the left side of the hull. Edge 1R bends downward. The square formed by edges 2R, 3R, and 4R rotates down and out at the rear of the hull. In mode 15, the motion of the right side of the vehicle is similar to mode 14. Edges 2L, 3L, and 4L behave the same as edges 2R, 3R, and 4R. The two sides twist inward simultaneously. As the sides twist in, the floor and roof are depressed downward. Mode 16 is similar to mode 15. The two sides have depressions formed in their centers as they twist. The forward portion of the right side is flapping in and out. The floor and roof motion are similar to mode 15 at lower relative amplitude.

Mode 17. Edge 1L and 2L bow down and out while edge 3L bows up and out. Edges 1R and 2R bow upward and inward while 3R bows up and inward. The floor twists while the front and rear edges of the cargo hatch bend up and down, out of phase with each other.

Modes 18–19. The center of the hull's left side is depressed while the unsupported front part of the right side flaps. The roof also bends between the commander's hatch and the cargo hatch. The left side of the hull in mode 19 is very similar to mode 18. The rectangle formed by edges 2R, 3R, and 4R rotates down and to the right. The roof between the commander's hatch and the cargo hatch rocks left and right.

Mode 20. Edges 3L and 4L bow inward and a depression forms in the plane between them. The rear portion of edge 1L bends outward slightly. Edges 1R, 2R, and 3R bow downward and outward. A large depression forms in the center of the floor. The roof panel between the commander's hatch and cargo hatch rocks side to side.

Mode 21. The center of the right side of the vehicle bows outward, pulling the adjacent edges with it. Edges 2L and 3L bow outward while edge 4L bows inward and downward. The roof behaves similarly to mode 19.

Mode 22. Edges 1L and 2L bow upward while edge 3L bows inward. A sinusoidal wave forms in the plane between edges 3R and 4R. The roof panels rock from front to back. The unsupported portion of the hull's right side flaps left and right.

Modes 23–24. Edges 1R, 2R, 3R, and 4R all bow toward the center of the vehicle. Edge 3L and 4L bow downward. Edge 1L bows downward and outward slightly. There is a depression in the plane formed by edges 3L and 4L. The roof panels rock front to back. Mode 24 is similar to mode 23. There is a depression in the plane formed by edges 3R and 4R.

Modes 25–27. The rear part of the right side of the hull is twisting upward and outward. The depressions in the left and right sides of the vehicle are in different longitudinal locations. The center rear part of the floor is depressed downward. Mode 26 is similar to mode 25, however, the roof around the commander's hatch bows upward in this mode. Mode 27 is similar to mode 26. The displacement around the commander's hatch is different.

4.6 Tight-Fitting Configuration, Composite Hull. The tight-fitting composite hull was instrumented identically to the tight-fitting aluminum hull. The extracted modal parameters appear in Table 6. The highest frequency RBM is less than 4 Hz. The next mode is at approximately 10 Hz. This mode involves primarily the engine moving independent of the hull. However, because there are no isolation blocks between the engine and the hull, the floor of the hull also exhibits some flexure. The next set of modes is around 20 Hz. This should provide enough separation between the elastic modes and the RBMs to decouple the two.

The MMIF appears in Figure 18, the four driving-point FRFs appear in Figure 19, and the MAC matrix appears in Figure 20. By inspection of the driving-point FRFs, the modes become very highly coupled above 60 Hz. Above 78 Hz, modes could not be extracted with reasonable accuracy. As the frequency increases, the difference between mode shapes becomes much smaller and more sensors are required to uniquely describe each mode.

Modes 1–6. Mode 1 is a roll RBM. Mode 2 is a pitch RBM. Modes 3 and 4 are noisy heave modes. Mode 5 is a longitudinal translation mode. Mode 6 is a roll mode combined with some transverse translation.

Modes 7–8. The forward portion of the floor beneath the engine/transmission is deflecting downward. Mode 8 has the same floor and engine motion as mode 7, however, the entire vehicle is rolling on a diagonal line from the front left corner to the rear right corner.

Table 6. Tight-Fitting Configuration, Composite Hull

Mode No.	Frequency (Hz)	Damping (percent critical)	Mode No.	Frequency (Hz)	Damping (percent critical)
1	1.2	3.55	17	44.1	0.31
2	1.9	2.04	18	46.2	2.58
3	2.4	1.99	19	48.4	3.22
4	2.4	1.75	20	52.7	2.50
5	3.3	1.73	21	56.4	0.29
6	3.6	2.30	22	58.5	1.83
7	10.8	2.62	23	60.2	1.24
8	18.5	2.45	24	64.2	1.43
9	20.6	2.24	25	64.4	1.66
10	24.3	0.42	26	65.0	1.44
11	29.2	1.85	27	68.2	1.86
12	32.3	2.36	28	68.7	1.52
13	34.8	2.66	29	70.2	2.05
14	35.3	2.07	30	74.5	0.99
15	39.4	2.28	31	74.8	1.90
16	43.2	0.77	32	78.9	1.27

Modes 9–10. The engine moves forward and backward while the entire vehicle pitches. The primary deflection occurs on the roof at the cargo hatch. The cargo hatch moves vertically and the adjacent roof moves with it. The commander's hatch also moves vertically in phase with the cargo hatch. The motion of mode 10 if very similar to mode 9, however, the roof deflection is centered farther forward.

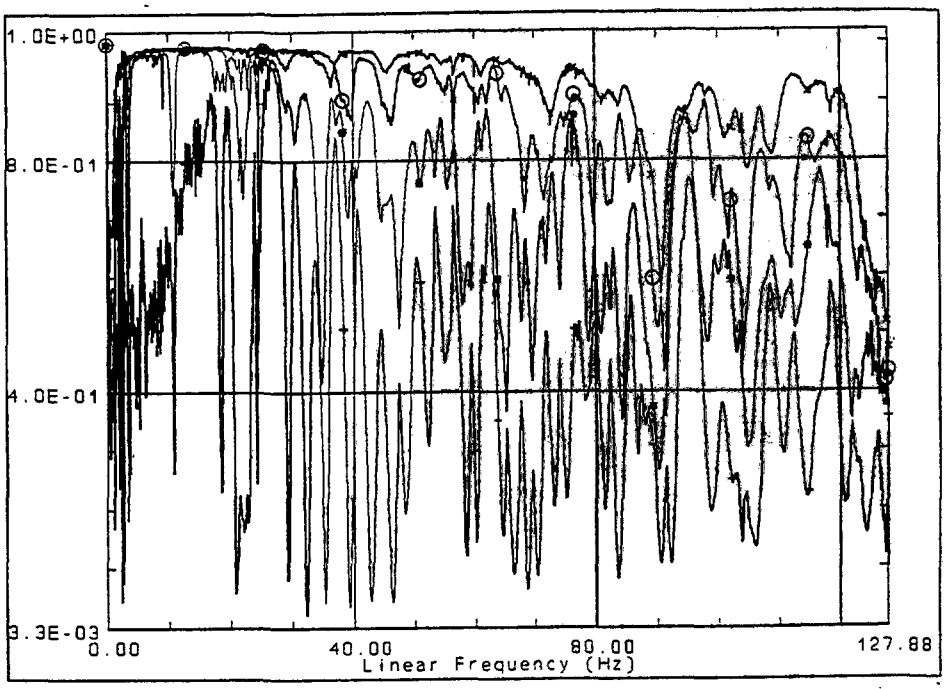

Figure 18. Tight-fitting configuration, composite hull MMIF.

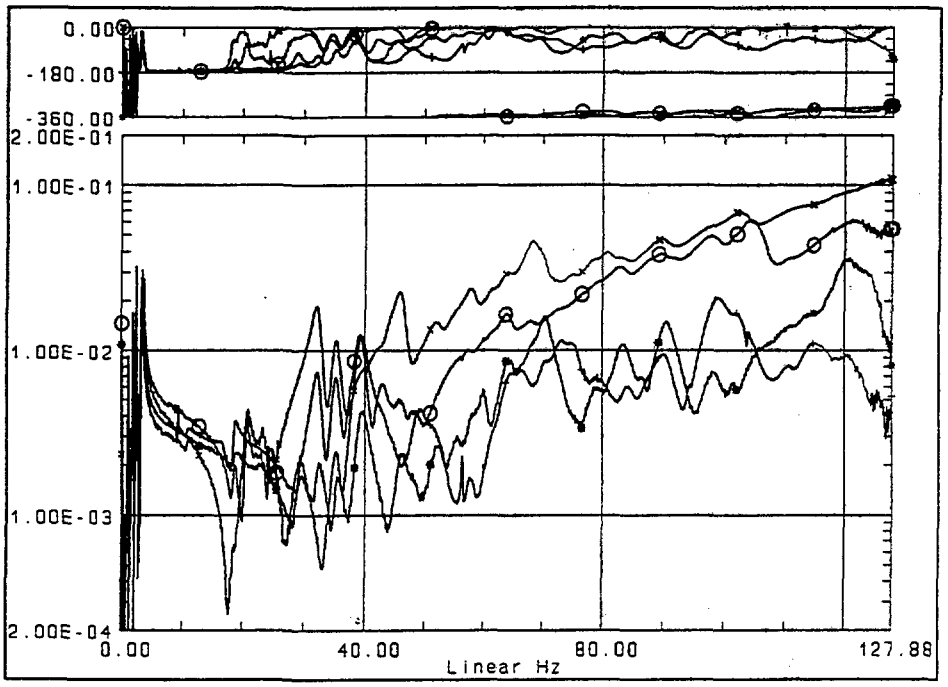

Figure 19. Tight-fitting configuration, composite hull driving-point FRFs.

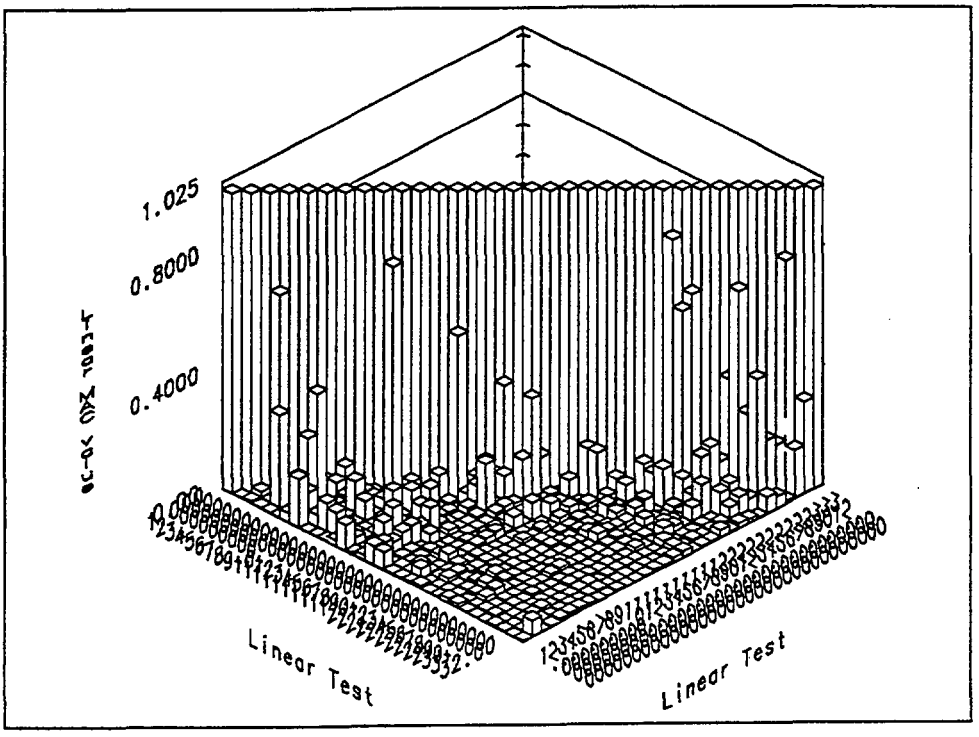

Figure 20. Tight-fitting configuration, composite hull MAC matrix.

Mode 11. The motion emanates primarily from the roof. The cargo hatch and commander's hatch are moving vertically. However, in this mode their motions are out of phase with each other.

Mode 12. This is primarily a torsional mode of the hull. The rear ramp, however, is rotating in-plane out of phase with the hull. The engine is moving vertically and the cargo hatch and commander's hatch rotate primarily from side to side.

Mode 13. The commander's hatch and the cargo hatch rock from front to back and the adjacent hull edges move with the respective hatch.

Mode 14. Mode 14 is an obvious torsional mode. The rear ramp moves with a small amplitude compared to the rear of the hull, but its motion is in phase with that of the hull.

Mode 15. The top of the hull translates sideways slightly while the commander's and cargo hatches rock side to side. The engine and top covers translate vertically while the rear ramp rotates slightly in-plane.

Mode 16. Mode 16 appears in Figure 21. This is also a torsional mode very similar to mode 14. The center of the commander's hatch has a large vertical displacement.

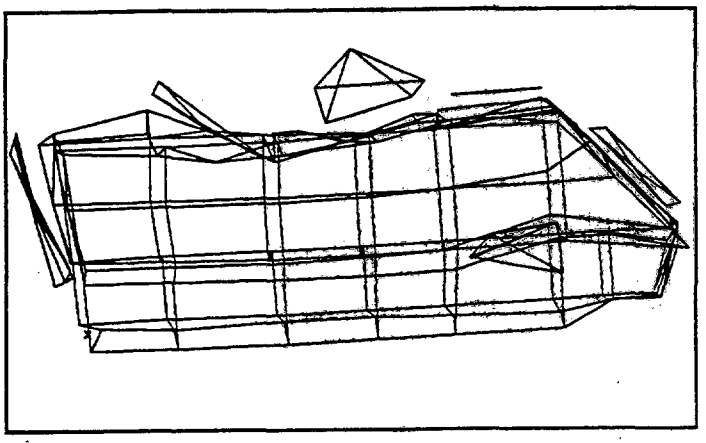

Figure 21. Tight-fitting configuration, composite hull, mode 16, 43.2 Hz.

Modes 17–18. The rear ramp rotates in-plane while the door in the ramp pivots on its hinges. The cargo hatch rocks side to side with its adjacent roof edges. Mode 18 exhibits the same motion in the rear ramp and in the cargo and commander's hatches. The engine and top covers also translate vertically. The engine cover motion includes a slight rotation as well.

Mode 19. The entire rear ramp and door rotate about their vertical axis. The cargo hatch rocks front to back while the commander's hatch center moves slightly. The engine cover and top cover rotate side to side, although they are out of phase with each other. Both covers also translate vertically.

Mode 20. The rear ramp bends slightly along a horizontal axis. The cargo hatch and commander's hatch rock side to side out of phase with each other. Edges 2L and 3L bow inward while the engine cover and top cover move similarly to their motion in mode 19.

Modes 21–23. The rear ramp rotates about its vertical axis and the engine cover rotates about its right edge. Mode 22 exhibits the same motion as mode 21, with the addition of several components. The driver's hatch translates front to rear as does the commander's hatch. Edge 1L, 2L, and 3L bow toward the center of the vehicle while edge 4L bows away from the center of the vehicle. Mode 23 includes the motion from mode 22 and adds a torsional motion as well. All of the roof hatches rock side to side.

Modes 24–25. Edges 1R, 2R, and 3R bow inward toward the center of the hull. The center of the right side is also depressed inward. Edges 1L and 2L bow downward while edge 3L bows upward. The center of the plane formed by edge 3L and 4L is depressed. The driver's hatch translates vertically. Mode 25 is very similar to mode 24, but the door in the rear ramp swings on its hinges.

Modes 26–27. The roof of the vehicle remains stationary while the hatches rock and translate. Edges 1L, 2L, and 3L bow toward the center of the vehicle while edges 1R, 2R, and 3R bow away from the center of the vehicle. The rear ramp translates along a diagonal line. Mode 27 adds a high-amplitude rocking of the commander's hatch and a vertical translation of the driver's hatch.

Mode 28. Edges 2L and 3L bend in an "S" shape while edge 4L bows downward. Edges 2R and 3R bow inward. The commander's and driver's hatches move in a manner similar to mode 27.

Modes 29–30. Edge 1L and 2L bow upward and inward while edges 3L and 4L bow downward and inward. The cargo hatch, commander's hatch, engine cover, and driver's hatch rock on a diagonal line. The door in the rear ramp moves slightly on its hinges. Mode 30 is similar to mode 29, but adds flexing motion of the rear of the roof around the cargo hatch.

Mode 31. Edges 2L and 3L bow outward while edge 4L bows inward and downward. Edge 1R, 2R, and 3R bow inward and upward. The roof flexes in transverse waves. The panel between the rear edge and cargo hatch, is out of phase with the panel between the commander's hatch and the cargo hatch. The roof hatches rock side to side.

Mode 32. Edges 1L and 2L bow upward while edges 3L and 4L bow downward. The center of the plane formed by edges 3L and 4L exhibits a depression. Edge 3R bows outward slightly. The roof hatches rock side to side and front to back on a diagonal line. The roof panels between the rear of the vehicle, the cargo hatch, and the commander's hatch twist along a transverse axis.

5. CONCLUSIONS

The modal parameters which were extracted provide a solid database through which the dynamic properties of the finite element model can be verified. The first several modes of the basic configurations are more accurate than the others. When validating the finite element model, the modeler should realize

that the damping values of the first several modes exhibited better convergence characteristics in the analysis than the higher frequency damping values.

The complexities revealed in this modal analysis serve to reinforce the importance of conducting an experimental validation of FE models. The basic configuration of each hull provides a significant database upon which the FE modeler can build. In addition to providing a means of validation for the FE model, this analysis also provides missing structural parameters, such as damping factors, to the FE modeler. The modeler can easily replicate the boundary conditions represented in this test and form a comparison between the experimental structure and the analytic model. Inconsistencies arising from this comparison can be used to validate or negate some of the assumptions that an FE modeler must make.

5.1 Metallic vs. Composite Hulls. The first elastic mode of the basic configurations of both hulls is extremely similar. For the metallic hull, this mode is at 43.3 Hz and has a damping factor of 0.21%, and for the composite hull the corresponding mode is at 27.5 Hz with a damping factor of 1.3%. This is a rather large difference in the dynamic properties of each hull. The composite hull is more compliant than the aluminum as evidenced by the lower modal frequency. The damping of the composite hull is also much greater than that of the metallic hull. The higher damping results from the composite hull having a higher material damping coefficient than the aluminum hull.

It is difficult to compare the two tight-fitting configurations. There is a much larger variety and combination of motions resulting from the various added components. A large factor in the dynamic properties of these components is their particular method and tightness of attachment to the hull. This facet of the structure changes each time a component is added to or removed from the hull. Therefore, this comparison would not provide much insight into the dynamic differences between the two tight-fitting configurations. These two analyses illustrate to the modeler how different components and attachment methods and tightnesses can affect the overall dynamics of the structure.

5.2 Basic vs. Tight-Fitting Configurations. As expected, the addition of 5,000 lbs of weight to the basic hull has a significant impact on its dynamic behavior. The number of modes increases for the tight-fitting configuration. This is an obvious result as the systems' dynamic motion increases in complexity as more components are added.

The mounting method of the drive-train causes the forward portion of the floor to participate in more modes in these configurations. Instead of mounting the drive-train on isolation blocks (as in the Bradley Fighting Vehicle), they are bolted directly to the hull. As a result, these components are unable to move independently of the hull.

5.3 Bradley Fighting Vehicle Comparison. The test and analysis which were performed on this M113 armored personnel carrier are very similar to the test and analysis which were performed previously on a Bradley Infantry Fighting Vehicle (BIFV). Both structures exhibited the same trend of increased damping for the composite material as well as a lower first elastic mode for the composite hull. Many of the modes in both vehicles (M113 and BIFV) involved a twisting of the hull along its longitudinal axis. The tight-fitting configuration of the M113 did not exhibit the distinct engine motion that the tight-fitting BIFV exhibited. The analysis of an additional vehicle serves to increase the size of the validation database from which a modeler of these types of structures may draw experience and knowledge.

INTENTIONALLY LEFT BLANK.

BIBLIOGRAPHY

Berman, M. S., and Li, T. H. "Modal Analysis of Bradley Fighting Vehicle (BFV): Prototype Composite Hull and Production Metallic Hull." ARL-TR-445, U.S. Army Research Laboratory, Aberdeen Proving Ground, MD, 1994.

Braun, S. Mechanical Signature Analysis: Theory and Applications. London: Harcourt Brace Jovanovich, 1986.

Brown, D. L., R. J. Allemang, and R. Zimmerman. "Parameter Estimation Techniques for Modal Analysis." Technical Paper Series 90221, Society of Automotive Engineers, Inc., 26 February–2 March 1979.

University of Cincinnati, Structural Dynamics Research Laboratory. "Advanced Shock Impact Mechanics Methodology for Armored Fighting Vehicles: Experimental Modal Analysis Data Acquisition for Composite and Aluminum Hull M113 Armored Personnel Carriers." U.S. Army Research Laboratory Contract DAAL01-93-R-9280/RH531A, Cincinnati, OH, 1993.

INTENTIONALLY LEFT BLANK.

APPENDIX:

FIRESTONE AIRMOUNT ISOLATOR DATA SHEET

INTENTIONALLY LEFT BLANK.

	Description	Order No.
Style 113 Two Ply Bellows	Blind nuts, 1/4 NPT	WO1-358-7103
	Blind nuts, 1/4 NPT, bumper	WO1-358-7104
	Blind nuts, 3/4 NPT	WO1-358-7101
	Blind nuts, 3/4 NPT, bumper	WO1-358-7109
	Steel button head bead rings, 1⅞ bolts, nuts, washers	WO1-358-7110
	Blind nuts, 1/8 NPT	WO1-753-7113
	Blind nuts, 1¼ NPT	WO1-753-7114
	Rubber Bellows Only	WO1-358-0135
Assembly weight ..... 14.5 lbs.		
Force to collapse to minimum height (@ 0 PSIG) ..... 17 lbs.		
Style 128 Four Ply Bellows	Blind nuts, 1/4 NPT	WO1-358-8151
	Blind nuts, 1/4 NPT, rubber bumper	WO1-358-8149
	Blind nuts, 3/4 NPT	WO1-358-8152
	Blind nuts, 3/4 NPT, rubber bumper	WO1-358-8150
	Rubber Bellows Only	WO1-358-0231

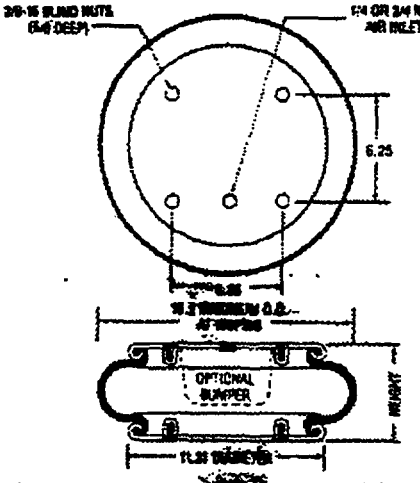

NOTE: This part is also available with bead rings (rather than end plates) SEE PAGE 6.

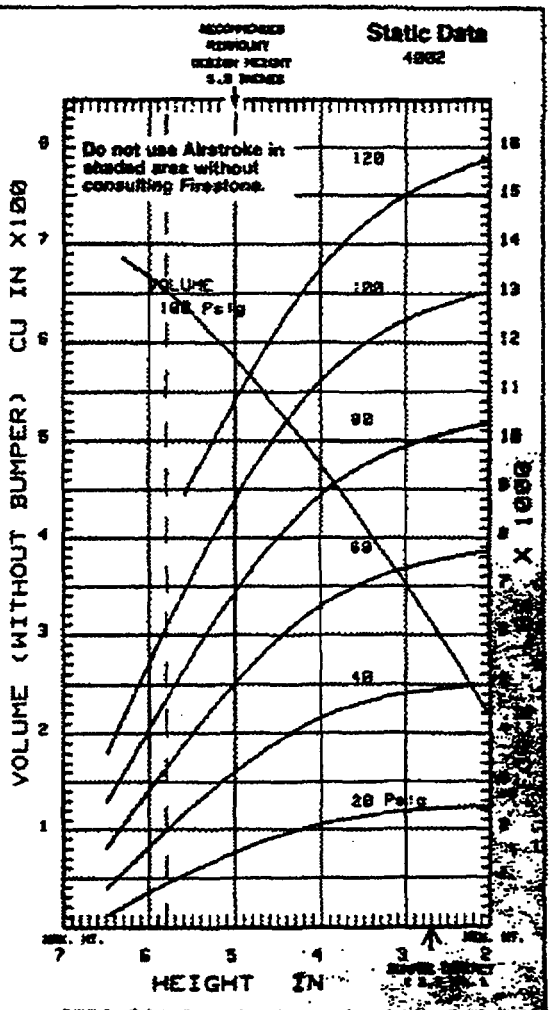

SEE PAGE 12 for instructions on how to use

Dynamic Characteristics at 5.0 in. Design Height (Required for Airmount isolator design only)				
Volume = 100 PSIG = 585 in³			Natural Frequency	
Gage Pressure (PSIG)	Load (lbs.)	Spring Rate (lbs./in.)	CPM	HZ
40	3,220	2,428	163	2.72
60	5,030	3,432	155	2.58
80	6,890	4,407	150	2.50
100	8,800	5,385	147	2.45

Force Table (Use for Airstroke actuator design)

Assembly Height (in.)	Volume @ 100 PSIG (in³)	Pounds Force @ 20 PSIG	@ 40 PSIG	@ 60 PSIG	@ 80 PSIG	@ 100 PSIG
5.0	585	1,540	3,220	5,030	6,890	8,800
4.0	477					
3.0	353	2,390	4,830	7,380	9,900	12,470

INTENTIONALLY LEFT BLANK.

NO. OF COPIES	ORGANIZATION
2	ADMINISTRATOR ATTN DTIC DDA DEFENSE TECHNICAL INFO CTR CAMERON STATION ALEXANDRIA VA 22304-6145
1	DIRECTOR ATTN AMSRL OP SD TA US ARMY RESEARCH LAB 2800 POWDER MILL RD ADELPHI MD 20783-1145
3	DIRECTOR ATTN AMSRL OP SD TL US ARMY RESEARCH LAB 2800 POWDER MILL RD ADELPHI MD 20783-1145
1	DIRECTOR ATTN AMSRL OP SD TP US ARMY RESEARCH LAB 2800 POWDER MILL RD ADELPHI MD 20783-1145
	ABERDEEN PROVING GROUND
5	DIR USARL ATTN AMSRL OP AP L (305)

NO. OF COPIES	ORGANIZATION
1	HQDA ATTN SARD TT DR F MILTON WASHINGTON DC 20310-0103
1	HQDA ATTN SARD TT MR J APPEL WASHINGTON DC 20310-0103
1	HQDA ATTN SARD TT MS C NASH WASHINGTON DC 20310-0103
1	HQDA ATTN SARD TR DR R CHAIT WASHINGTON DC 20310-0103
1	HQDA ATTN SARD TR MS K KOMINOS WASHINGTON DC 20310-0103
1	DIR ATTN AMSRL CP CA D SNIDER US ARMY RESEARCH LABORATORY 2800 POWDER MILL RD ADELPHI MD 20783
6	DIR ATTN AMSRL MA P L JOHNSON B HALPIN T CHOU AMSRL MA PA D GRANVILLE W HASKELL AMSRL MA MA G HAGNAUER US ARMY RESEARCH LABORATORY WATERTOWN MA 02172-0001
4	CDR ATTN SMCAR FSE T GORA E ANDRICOPOULOS B KNUTELSKY A GRAF US ARMY ARDEC PCTNY ARSNL NJ 07806-5000
3	CDR ATTN SMCAR TD R PRICE V LINDER T DAVIDSON US ARMY ARDEC PCTNY ARSNL NJ 07806-5000
1	CDR ATTN F MCLAUGHLIN US ARMY ARDEC PCTNY ARSNL NJ 07806-5000
5	CDR ATTN SMCAR CCH T S MUSALLI P CHRISTIAN R CARR N KRASNOW US ARMY ARDEC PCTNY ARSNL NJ 07806-5000
1	CDR ATTN SMCAR CCH V E FENNELL US ARMY ARDEC PCTNY ARSNL NJ 07806-5000
1	CDR ATTN SMCAR CCH J DELORENZO US ARMY ARDEC PCTNY ARSNL NJ 07806-5000
2	CDR ATTN SMCAR CC J HEDDERICH COL SINCLAIR US ARMY ARDEC PCTNY ARSNL NJ 07806-5000
1	CDR ATTN SMCAR CCH P J LUTZ US ARMY ARDEC PCTNY ARSNL NJ 07806-5000
2	CDR ATTN SMCAR FSA M D DEMELLA F DIORIO US ARMY ARDEC PCTNY ARSNL NJ 07806-5000

NO. OF COPIES	ORGANIZATION
1	CDR ATTN SMCAR FSA C SPINELLI US ARMY ARDEC PCTNY ARSNL NJ 07806-5000
11	DIR ATTN SMCAR CCB C KITCHENS J KEANE J BATTAGLIA J VASILAKIS G FRIAR T SIMKINS V MONTVORI J WRZOCHALSKI G D'ANDREA R HASENBEIN SMCAR CCB R S SOPOK WATERVLIET NY 12189
1	CDR ATTN SMCWV QAE Q C HOWD BLDG 44 WATERVLIET ARSNL WATERVLIET NY 12189-4050
1	CDR ATTN SMCWV SPM T MCCLOSKEY BLDG 25/3 WATERVLIET ARSNL WATERVLIET NY 12189-4050
1	CDR ATTN SMCWV QA QS K INSCO WATERVLIET NY 12189-4050
1	CDR ATTN AMSMC PBM K US ARMY ARDEC PROD BASE MODRN ACT PCTNY ARSNL NJ 07806-5000
1	CDR ATTN STRBE JBC C KOMINOS US ARMY BELVOIR RD&E CTR FT BELVOIR VA 22060-5606
1	US ARMY COLD REGIONS RSRCH AND ENGRG LAB ATTN P DUTTA 72 LYME RD HANOVER NH 03755

NO. OF COPIES	ORGANIZATION
1	DIR ATTN AMSRL WT L D WOODBURY US ARMY RESEARCH LABORATORY 2800 POWDER MILL RD ADELPHI MD 20783-1145
3	CDR ATTN AMSMI RD W MCCORKLE AMSMI RD ST P DOYLE AMSMI RD ST CN T VANDIVER US ARMY MISSILE COMMAND REDSTONE ARSNL AL 35898
2	DIR ATTN ANDREW CROWSON J CHANDRA US ARMY RESEARCH OFFICE MATH & COMPUTER SCI DIV PO BOX 12211 RSRCH TRI PK NC 27709-2211
1	US ARMY RESEARCH OFFICE ATTN G ANDERSON ENGRG SCI DIV PO BOX 12211 RSRCH TRI PK NC 27709-2211
2	PROJECT MANAGER SADARM PCTNY ARSNL NJ 07806-5000
2	PROJECT MANAGER ATTN SFAE AR TMA COL BREGARD C KIMKER TANK MAIN ARMAMENT SYSTEMS PCTNY ARSNL NJ 07806-5000
3	PROJECT MANAGER ATTN SFAE AR TMA MD H YUEN J MCGREEN R KOWALSKI TANK MAIN ARMAMENT SYSTEMS PCTNY ARSNL NJ 07806-5000
2	PROJECT MANAGER ATTN SFAE AR TMA MS R JOINSON D GUZIEWICZ TANK MAIN ARMAMENT SYSTEMS PCTNY ARSNL NJ 07806-5000

NO. OF COPIES	ORGANIZATION
1	PROJECT MANAGER ATTN SFAE AR TMA MP W LANG TANK MAIN ARMAMENT SYSTEMS PCTNY ARSNL NJ 07806-5000
2	PEO ARMAMENTS ATTN SFAE AR PM D ADAMS T MCWILLIAMS PCTNY ARSNL NJ 07806-5000
1	PEO FIELD ARTILLERY SYSTEMS ATTN SFAE FAS PM H GOLDMAN PCTNY ARSNL NJ 07806
4	PROJECT MANAGER AFAS ATTN LTC D ELLIS G DELCOCO J SHIELDS B MACHAK PCTNY ARSNL NJ 07806-5000
2	CDR ATTN J KELLY B WILCOX DARPA 3701 NORTH FAIRFAX DR ARLINGTON VA 22203-1714
2	CDR ATTN WL FIV A MAYER WRIGHT PATTERSON AFB DAYTON OH 45433
2	NASA LANGLEY RSRCH CTR ATTN AMSRL VS W ELBER F BARLETT JR MAIL STOP 266 HAMPTON VA 23681-0001
2	NAVAL SURFACE WARFARE CTR DAHLGREN DIVISION CODE G33 DAHLGREN VA 22448
1	NAVAL RESEARCH LABORATORY ATTN I WOLOCK CODE 6383 WASHINGTON DC 20375-5000

NO. OF COPIES	ORGANIZATION
1	OFFICE OF NAVAL RESEARCH ATTN YAPA RAJAPAKSE MECH DIV CODE 1132SM ARLINGTON VA 22217
1	NAVAL ORDNANCE STATION ATTN D HOLMES ADVANCED SYSTEMS TECHNOLOGY BR CODE 2011 LOUISVILLE KY 40214-5245
1	DAVID TAYLOR RESEARCH CTR ATTN J CORRADO CODE 1702 SHIP STRUCT AND PROT DEPT BETHESDA MD 20814
2	DAVID TAYLOR RESEARCH CTR ATTN R ROCKWELL W PHYILLAIER BETHESDA MD 20814
5	DIR ATTN R CHRISTENSEN S DETERESA W FENG F MAGNESS M FINGER LAWRENCE LIVERMORE NAT LAB PO BOX 808 LIVERMORE CA 94550
1	DIR ATTN D RABERN LOS ALAMOS NATIONAL LAB MEE 13 MAIL STOP J 576 PO BOX 1633 LOS ALAMOS NM 87545
1	OAK RIDGE NATIONAL LAB ATTN R M DAVIS PO BOX 2008 OAK RIDGE TN 37831-6195
1	PACIFIC NORTHWEST LAB ATTN M SMITH PO BOX 999 RICHLAND WA 99352

NO. OF COPIES	ORGANIZATION
6	DIR ATTN C ROBINSON G BENEDETTI W KAWAHARA K PERANO D DAWSON P NIELAN SANDIA NATIONAL LABS APPLIED MECHANICS DEPT DIV 8241 PO BOX 969 LIVERMORE CA 94550-0096
1	DREXEL UNIVERSITY ATTN ALBERT S D WANG 32ND AND CHESTNUT ST PHILADELPHIA PA 19104
2	NORTH CAROLINA STATE UNIVERSITY ATTN W RASDORF L SPAINHOUR CIVIL ENGRG DEPT PO BOX 7908 RALEIGH NC 27696-7908
1	PENNSYLVANIA STATE UNIVERSITY ATTN DAVID W JENSEN 223 N HAMMOND UNIVERSITY PARK PA 16802
1	PENNSYLVANIA STATE UNIVERSITY ATTN RICHARD MCNITT 227 HAMMOND BLDG UNIVERSITY PARK PA 16802
1	PENNSYLVANIA STATE UNIVERSITY ATTN RENATA S ENGEL 245 HAMMOND BLDG UNIVERSITY PARK PA 16802
1	PURDUE UNIVERSITY ATTN C T SUN SCHOOL OF AERO & ASTRO W LAFAYETTE IN 47907-1282
1	STANFORD UNIVERSITY ATTN S TSAI DEPT OF AERONAUTICS AND AEROBALLISTICS DURANT BLDG STANFORD CA 94305

NO. OF COPIES	ORGANIZATION
1	UCLA ATTN H THOMAS HAHN MANE DEPT ENGRG IV LOS ANGELES CA 90024-1597
2	UNIVERSITY OF DAYTON RSRCH INST ATTN RAN Y KIM AJIT K ROY 300 COLLEGE PK AVE DAYTON OH 45469-0168
1	UNIVERSITY OF DAYTON ATTN JAMES M WHITNEY 300 COLLEGE PK AVE DAYTON OH 45469-0240
2	UNIVERSITY OF DELAWARE ATTN J GILLESPE M SANTARE CENTER FOR COMPOSITE MATERIALS 201 SPENCER LABORATORY NEWARK DE 19716
1	UNIVERSITY OF ILLINOIS AT URBANA CHAMPAIGN ATTN J ECONOMY NAT CTR FOR COMPOSITE MAT RSRCH 216 TALBOT LAB 104 S WRIGHT ST URBANA IL 61801
1	UNIVERSITY OF KENTUCKY ATTN LYNN PENN 763 ANDERSON HALL LEXINGTON KY 40506-0046
1	THE UNIVERSITY OF TEXAS AT AUSTIN CTR FOR ELECTROMECHANICS ATTN J PRICE 10100 BURNET RD AUSTIN TX 78758-4497
1	UNIVERSITY OF UTAH ATTN S SWANSON DEPT OF MECHL AND INDUST ENGRG SALT LAKE CITY UT 84112
2	VIRGINIA POLYTECHNICAL INST AND STATE UNIVERSITY ATTN MICHAEL W HYER KENNETH L REIFSNIDER DEPT OF ESM BLACKSBURG VA 24061-0219

NO. OF COPIES	ORGANIZATION
1	AAI CORPORATION ATTN J HEBERT PO BOX 126 HUNT VALLEY MD 21030-0126
1	ARMTEC DEFENSE PRODUCTS ATTN STEVE DYER 85 901 AVE 53 PO BOX 848 COACHELLA CA 92236
2	ADVANCED COMPOSITE MATERIALS CORP ATTN P HOOD J RHODES 1525 S BUNCOMBE RD GREER SC 29651-9208
6	ALLIANT TECHSYSTEMS INC ATTN C CANDLAND J BODE L OSGOOD R BURETTA R BECKER M SWENSON 600 SECOND ST HOPKINS MN 55343
1	AMOCO PERFORMANCE PRODUCTS INC ATTN M MICHNO JR 4500 MCGINNIS FERRY RD ALPHARETTA GA 30202-3944
1	APPLIED COMPOSITES ATTN W GRISCH 333 N SIXTH ST ST CHARLES IL 60174
1	BRUNSWICK DEFENSE ATTN T HARRIS STE 410 1745 JEFFERSON DAVIS HWY ARLINGTON VA 22202
1	CHAMBERLAIN MANUFACTURING CORP ATTN T LYNCH RSRCH AND DEV DIV PO BOX 2335 550 ESTHER ST WATERLOO IA 50704

NO. OF COPIES	ORGANIZATION
1	CHAMBERLAIN MANUFACTURING CORP ATTN M TOWNSEND RSRCH AND DEV DIV PO BOX 2545 550 ESTHER ST WATERLOO IA 50704
1	CUSTOM ANALYTICAL ENGRG SYS INC ATTN A ALEXANDER STAR ROUTE BOX 4A FLINTSTONE MD 21530
1	GENERAL DYNAMICS ATTN D BARTLE LAND SYSTEMS DIVISION PO BOX 1901 WARREN MI 48090
3	HERCULES INC ATTN R BOE F POLICELLI J POESCH PO BOX 98 MAGNA UT 84044
3	HERCULES INC ATTN G KUEBELER J VERMEYCHUK B MANDERVILLE JR HERCULES PLAZA WILMINGTON DE 19894
1	HEXCEL ATTN M SHELENDICH 11555 DUBLIN BLVD PO BOX 2312 DUBLIN CA 94568-0705
1	IAP RESEARCH INC ATTN A CHALLITA 2763 CULVER AVE DAYTON OH 45429
2	INST FOR ADVANCED TECHLGY ATTN T KIEHNE H FAIR P SULLIVAN 4030-2 W BRAKER LANE AUSTIN TX 78759

NO. OF COPIES	ORGANIZATION
1	INTEGRATED COMPOSITE TECHNOLOGIES ATTN H PERKINSON JR PO BOX 397 YORK NEW SALEM PA 17371-0397
1	INTERFEROMETRICS INC ATTN R LARRIVA VICE PRESIDENT 8150 LEESBURG PIKE VIENNA VA 22100
2	KAMAN SCIENCES CORP ATTN D ELDER T HAYDEN PO BOX 7463 COLORADO SPRINGS CO 80933
3	LORAL VOUGHT SYSTEMS ATTN G JACKSON K COOK L L HADDEN 1701 W MARSHALL DR GRAND PRAIRIE TX 75051
2	MARTIN MARIETTA CORP ATTN P DEWAR L SPONAR 230 E GODDARD BLVD KING OF PRUSSIA PA 19406
2	OLIN CORPORATION ATTN E STEINER B STEWART FLINCHBAUGH DIV PO BOX 127 RED LION PA 17356
1	OLIN CORPORATION ATTN L WHITMORE 10101 9TH ST N ST PETERSBURG FL 33702
1	RENNSAELER POLYTECHNIC INST ATTN R B PIPES TROY NY 12181
1	SPARTA INC ATTN J GLATZ 9455 TOWNE CENTRE DR SAN DIEGO CA 92121-1964

NO. OF COPIES	ORGANIZATION
2	UNITED DEFENSE LP ATTN P PARA G THOMAS 1107 COLEMAN AVE BOX 367 SAN JOSE CA 95103
	ABERDEEN PROVING GROUND
63	DIR, USARL ATTN: AMSRL-CI, W. MERMAGEN AMSRL-CI-C, W. STUREK AMSRL-CI-S, A. MARK AMSRL-IS-TP, R. KASTE AMSRL-SL-B, P. DIETZ (328) AMSRL-SL-BA, J. WALBERT (1065) AMSRL-SL-BL, D. BELY (328) AMSRL-SL-I, D. HASKILL (1065) AMSRL-WT-P, A. HORST AMSRL-WT-PA, T. MINOR C. LEVERITT D. KOOKER AMSRL-WT-PB, E. SCHMIDT P. PLOSTINS AMSRL-WT-PC, R. FIFER AMSRL-WT-PD, B. BURNS W. DRYSDALE K. BANNISTER T. BOGETTI J. BENDER R. MURRAY R. KIRKENDALL T. ERLINE D. HOPKINS S. WILKERSON D. HENRY R. KASTE L. BURTON J. TZENG R. LIEB G. GAZONAS M. LEADORE C. HOPPEL

NO. OF
COPIES ORGANIZATION

AMSRL-WT-PD(ALC),
A. ABRAHAMIAN
K. BARNES
M. BERMAN
H. DAVISON
A. FRYDMAN
T. LI
W. MCINTOSH
E. SZYMANSKI
AMSRL-WT-T,
W. MORRISON
AMSRL-WT-TA,
W. GILLICH
W. BRUCHEY
AMSRL-WT-TC,
K. KIMSEY
R. COATES
W. DE ROSSET
AMSRL-WT-TD,
D. DIETRICH
G. RANDERS-PEHRSON
J. HUFFINGTON
A. DAS GUPTA
J. SANTIAGO
AMSRL-WT-W, C. MURPHY
AMSRL-WT-WA,
H. ROGERS
B. MOORE
A. BARAN
AMSRL-WT-WB,
F. BRANDON
W. D'AMICO
AMSRL-WT-WC,
J. ROCCHIO
AMSRL-WT-WD,
A. ZIELINSKI
J. POWELL
AMSRL-WT-WE,
J. TEMPERLEY
J. THOMAS

USER EVALUATION SHEET/CHANGE OF ADDRESS

This Laboratory undertakes a continuing effort to improve the quality of the reports it publishes. Your comments/answers to the items/questions below will aid us in our efforts.

1. ARL Report Number ARL-MR-246 Date of Report August 1995

2. Date Report Received _____

3. Does this report satisfy a need? (Comment on purpose, related project, or other area of interest for which the report will be used.) _____

4. Specifically, how is the report being used? (Information source, design data, procedure, source of ideas, etc.) _____

5. Has the information in this report led to any quantitative savings as far as man-hours or dollars saved, operating costs avoided, or efficiencies achieved, etc? If so, please elaborate. _____

6. General Comments. What do you think should be changed to improve future reports? (Indicate changes to organization, technical content, format, etc.) _____

CURRENT ADDRESS

_____
Organization

_____
Name

_____
Street or P.O. Box No.

_____
City, State, Zip Code

7. If indicating a Change of Address or Address Correction, please provide the Current or Correct address above and the Old or Incorrect address below.

OLD ADDRESS

_____
Organization

_____
Name

_____
Street or P.O. Box No.

_____
City, State, Zip Code

(Remove this sheet, fold as indicated, tape closed, and mail.)
(DO NOT STAPLE)

DEPARTMENT OF THE ARMY

OFFICIAL BUSINESS

NO POSTAGE
NECESSARY
IF MAILED
IN THE
UNITED STATES

BUSINESS REPLY MAIL
FIRST CLASS PERMIT NO 0001,APG,MD

POSTAGE WILL BE PAID BY ADDRESSEE

DIRECTOR
U.S. ARMY RESEARCH LABORATORY
ATTN: AMSRL-WT-PD
ABERDEEN PROVING GROUND, MD 21005-5066